IEEE Access
Multidisciplinary | Rapid Review | Open Access Journal

Received March 19, 2019, accepted May 17, 2019, date of publication June 19, 2019, date of current version July 17, 2019.

Digital Object Identifier 10.1109/ACCESS.2019.2923787

Analyzing Competition and Cooperation Dynamics of the Aerial mmWave Access Market

OLGA GALININA[1], LEONARDO MILITANO[2], SERGEY ANDREEV[1], ALEXANDER PYATTAEV[3,4], KERSTIN JOHNSSON[5], ANTONINO ORSINO[2], GIUSEPPE ARANITI[2], ANTONIO IERA[2], MISCHA DOHLER[6], AND YEVGENI KOUCHERYAVY[1]

[1]Unit of Electrical Engineering, Tampere University, 33720 Tampere, Finland
[2]ARTS Laboratory, DIIES Department, University Mediterranea of Reggio Calabria, 89124 Reggio Calabria, Italy
[3]YL-Verkot Oy, Tampere, Finland
[4]Peoples' Friendship University of Russia (RUDN University), 117198 Moscow, Russia
[5]Intel Corporation, Santa Clara, CA 95052, USA
[6]Department of Informatics, King's College London, London WC2R 2LS, U.K.

Corresponding author: Olga Galinina (olga.galinina@tuni.fi)

This work was supported in part by the "RUDN University Program 5-100" and in part by the RFBR under Grant 17-07-00845 and Grant 19-07-00933. The work of O. Galinina was supported in part by the Academy of Finland through the projects CROWN and WiFiUS, in part by the personal Jorma Ollila Grant from the Nokia Foundation, and in part by the Finnish Cultural Foundation. The work of S. Andreev was supported by the Academy of Finland through the Research Fellow project RADIANT and project PRISMA. This work was developed within the framework of the COST Action CA15104 IRACON.

ABSTRACT Cellular operators have always relied on static deployments for providing wireless access. However, even the emerging fifth-generation (5G) networks may face difficulty in supporting the increased traffic demand with a rigid, fixed infrastructure without substantial over-provisioning. This is particularly true for spontaneous large-scale events that require service providers to augment the capacity of their networks quickly. Today, the use of aerial devices equipped with high-rate radio access capabilities has the potential to offer the much needed "on-demand" capacity boost. Conversely, it also threatens to rattle the long-standing business strategies of wireless operators, especially as the "gold rush" for cheaper millimeter wave (mmWave) spectrum lowers the market entry barriers. However, the intricate structure of this new market presently remains a mystery. This paper sheds light on competition and cooperation behavior of dissimilar aerial mmWave access suppliers, concurrently employing licensed and license-exempt frequency bands, by modeling a vertically differentiated market where customers have varying preferences in price and quality. To understand viable service provider strategies, we begin by constructing the Nash equilibrium for the initial market competition by employing the Bertrand and Cournot games. We then conduct a unique assessment of short-term market dynamics, where licensed-band service providers may cooperate to improve their competitive positions against the unlicensed-band counterparts intruding on the market. Our analysis studies the effects of various market interactions, price-driven demand evolution, and dynamic profit balance in this novel type of ecosystem.

INDEX TERMS 5G systems, mmWave technology, aerial access points, UAV, competition and cooperation behavior, vertically differentiated market, Bertrand and Cournot models, dynamic games.

I. INTRODUCTION AND BACKGROUND

A. 5G DEVELOPMENT UPDATE

The initial stage of the global research on fifth-generation (5G) radio access systems has essentially been completed, and the respective standardization by 3GPP is progressing at full speed with the first 5G New Radio Release 15 frozen in June 2018 [1]. The 5G specifications address an extreme variation of scenarios that have difficulty to be served with the previous generations of radio technologies, which are commonly divided into three categories: (i) massive Internet of Things, (ii) mission-critical services, and (iii) enhanced mobile broadband (eMBB) use cases [2], [3]. Each of the three assumes a specific set of stringent connectivity

The associate editor coordinating the review of this manuscript and approving it for publication was Yulong Zou.

requirements, some of which are challenging to materialize without moving up in frequency to millimeter-wave (mmWave) spectrum.

Although the conceptual adoption of mmWave frequencies has been around for several years, practical bandwidth expansion campaigns have only begun recently with mmWave equipment presently available for both licensed and unlicensed spectrum (see, e.g., Qualcomm QTM052 mmWave antenna module[1] announced in 2018 and earlier Acelink BR-6774AD[2]). Unlicensed mmWave bands at 60 GHz (controlled by IEEE 802.11ad and 802.11ay standards [4], [5]) have started to be employed by commercial Wi-Fi products, while for the licensed cellular use, the FCC finalized bidding for 24 and 28 GHz (both licenses commenced in November 2018). All of this – further supported by industrial implementation efforts – carries a promise that first commercial 5G deployments will operate in mmWave bands under 40 GHz already by the end of 2019.

B. DYNAMIC 5G ACCESS INFRASTRUCTURE

Due to specific radio propagation conditions at extremely high frequencies, the network providers willing to enable mmWave connectivity are expected to deploy ultra-dense infrastructures [6], [7]. In this course, throughout more than 40 years of its history, the cellular industry has primarily relied on static radio access network (RAN) infrastructures, where it takes a considerable time to deploy additional access points. Hence, service providers are actively seeking alternative methods as well as technologies and system design options that enable non-rigid placement of access nodes to better accommodate the varying space-time user demand [8]. It has been understood recently that unmanned aerial vehicles (UAVs) equipped with wireless transceivers have the potential to bring the access supply to where the demand is, by enabling more flexible and on-demand communication networks [9], which may soon lay the foundation for truly dynamic RAN solutions [10]. Subject to suitable regulatory frameworks [11], UAVs can not only augment wireless capacity and coverage by meshing with conventional RAN systems and dynamically ''patching'' them where needed, but also share network infrastructure with, e.g., cargo delivery drones, thus bridging across transportation and communication markets.

As futuristic as it may sound, today's UAVs can already be equipped with mmWave access capabilities facilitated by the cost reduction and miniaturization of electronic components.[3] One of the key challenges in UAV-based radio access is in the respective power consumption, and thus in the UAV flight times, which is being addressed by numerous flight tests and trials for microwave UAV deployments. The mmWave test flights include the famous Facebook Aquila project[4] with a circling Cessna aircraft that provides 40 Gbps data rates as well as the project by the Defense Advanced Research Projects Agency (DARPA) deploying a self-organizing mmWave network over RQ-7 Shadow drones[5] with the data rates of up to 1 Gbps and the flight times of up to 9 hours.

Owing to their agility and mobility, rapidly deployable drone small cells (or simply *drone cells*) will be particularly useful in 5G networks during unexpected and temporary events, such as large-scale mass outdoor happenings that create unpredictable access demand fluctuations. The examples of such scenarios, as envisioned by [12], include an open-air festival or a marathon use case with very high densities of users and their connected handheld or wearable devices that altogether produce vast amounts of aggregated traffic. In such areas of interest where conventional RAN infrastructure may be sparse and under-dimensioned, aerial access systems can promptly assist the existing cellular networks by offering the much-needed capacity boost.

Fundamentally, the use of drone cells for ''on-demand'' RAN densification might in the future lead to very different dimensioning of our networks where they are no longer planned for peak loads but instead provisioned for median loading. Many important challenges have already been resolved to advance this thinking [13], [14], and in fact, Google has already announced their strategy to offer aerial wireless access in emerging markets.[6] Inspired by these promising scientific, technological, and business advances, *in this work* we put forward the vision of aerial mmWave access networks employing mmWave RAT in high demand and overloaded situations. We argue that mmWave technology is particularly attractive for aerial access due to many factors, such as simpler air interface design exploiting large bandwidths [15] and higher chances of having a line-of-sight link to the user on the ground, which is crucial for efficient mmWave operation.

As follows from the above, aerial mmWave access systems may soon deliver very high spectral efficiencies and ultra-broadband service experience, hence attracting various operators to leverage the cheaper mmWave spectrum. Although perspectives and technical challenges associated with aerial mmWave cellular networks have recently received significant attention from the research community [14], [16]–[18], the structure of this *unique market* is not nearly well understood and remains in immediate need of a comprehensive research perspective. Fortunately, the broad field of game theory supplies us with a rich set of tools to address its dynamics and study the intricate interactions between the existing players that may want to adapt their respective business strategies as well as the new

[1] https://www.qualcomm.com/products/qtm052-mmwave-antenna-modules

[2] http://www.acelink.com.tw/BR-6774AD.html

[3] The size of an antenna array may be estimated at around 3.75 cm for 60 GHz and 8 cm for 28 GHz (assuming a 16×16 uniform rectangular array and a half-wavelength inter-element distance)

[4] https://code.fb.com/connectivity/high-altitude-connectivity-the-next-chapter/

[5] https://www.darpa.mil/news-events/2014-04-07

[6] Alan Weissberger, ''Google's Internet Access for Emerging Markets''

market stakeholders. We continue with a review of our selected game-theoretic mechanisms in what follows.

C. GAME THEORY FOR AERIAL mmWave MARKET

The emerging 5G mmWave access market structure and interactions remain a vastly unexplored area as of today. Accordingly, various market players concurrently employing licensed and license-exempt mmWave spectrum will have to take into account the evolved expectations of their customers when offering new services. In this paper, we target careful game-theoretical modeling of viable business strategies in the aerial mmWave access market by systematically bringing into focus the aspects of the quality of service (QoS) and pricing, mindful of customer preferences. While applying advanced game theory tools [19] to wireless networking [20]–[22], [22] and, in particular, to the modeling and design of aerial networks [23] has been addressed in the existing literature, analysis of the dynamics of emerging mmWave licensed/unlicensed access represents an unexplored direction.

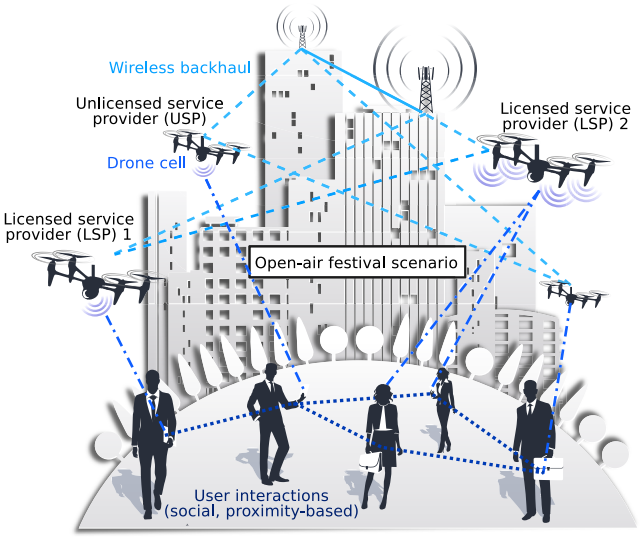

FIGURE 1. Our motivating scenario with 5G drone cells.

Our first line of research considers an *oligopoly* setting where several licensed-band service providers (LSPs) enter the aerial mmWave access market and compete with each other to maximize their profits (see Fig. 1). In the past, market competition and pricing models have already attracted significant attention across the wireless community, as reported in [24] and [25]. To the best of our knowledge, however, no prior contribution in the existing literature on game theory has been considering *vertical differentiation* in the context of wireless networking where market players differentiate their products in terms of quality, as was studied in [26], [27], and [28].

This methodology is particularly interesting for the purposes of our analysis since [26] showed that for some parameters the game has a unique subgame perfect equilibrium at which only two players enter the market. Furthermore, these two suppliers choose to offer differentiated products and earn positive profits at equilibrium (if the production costs are disregarded). Different from the work in [26], we assume that the LSPs have already decided to enter the market and are instead interested in defining the optimal quality of their products as well as the corresponding prices/quantities [29]. Moreover, we provide general reasoning for the case of an arbitrary number of participants.

Therefore, our methodology at its initial stage studies market equilibria in which the LSPs first determine the specification of their offered products (i.e., mobile subscriptions) and then decide on the prices or the quantities of the products they sell according to a *Bertrand* or a *Cournot* competition model, respectively [30]. Another finding of this paper is in understanding how the outcome of the initial LSP competition is influenced by customer preferences (so-called *taste parameter*) willing to pay more or less for a higher quality product. After that, we introduce another entity into our system, an unlicensed-band service provider (USP) operating in the free-to-use mmWave spectrum, and then study the *dynamics* of the resulting market.

At the dynamic stage of our considered game, the customers are allowed to prefer the USP to the LSP for wireless access services, while previously inactive users can activate to connect to the USP. The decision strategy of the customers is tightly coupled with their individual *utility* perception, and the resulting user decisions determine the *strategy revision protocol* [31]. The latter is captured in our methodology as a combination of different subjective and social factors, such as ''curiosity'', ''dissatisfaction'', and ''gossiping''. In practice, the competing market players attempt to find countermeasures against customer decisions that might penalize their profits. While for the USP we model its ability to adapt the offered price over time according to the user choices, the LSPs do not have such luxury as they are bound by a long-term contractual agreement with their customers.

Correspondingly, the LSPs have to seek ways to maximize the chances of meeting their service-level agreements (SLAs) and thus prevent users from changing the provider *in the long run*. To this aim, we advocate the adoption of long-term cooperative agreements between the LSPs to improve the QoS perception levels for their customers. Such cooperation is particularly helpful if a customer could be served by an assisting LSP at much higher spectral efficiency. Our analysis shows that these forms of cooperation between the LSPs improve their profits as compared to the non-cooperative case. Then, the question is how to share the surplus among the cooperating players, which requires *fairness*-centric game-theoretic solutions [32]. In this work, we adopt the widely-accepted Shapley value [33] for its intrinsic capability to capture the contributions of individual players in a coalition [34].

Finally, we note that market evolution and price dynamics were investigated in other contexts as well, including heterogeneous small cell networks [35] and advanced offloading techniques [36]. Evolutionary games [37], [38] have also been receiving attention in the literature, with applications to competing wireless operators [39] and user groups sharing

the limited access bandwidth [40]. In contrast to the past work, our game formulations uniquely study the evolution of market shares for several LSPs and one USP according to the customer decisions as well as the ability of the USP to adapt its pricing strategy over time. Technically, we construct a system of differential equations that characterize the dynamics of our market by analyzing the situations when the LSPs avoid or engage into cooperation while competing with the USP.

D. CONTRIBUTIONS OF THIS WORK

We envision that the aerial mmWave access technologies will play a pivotal role in the emerging 5G market. To leverage their full potential, they will need to be accompanied by new powerful methodologies able to capture the intricate market dynamics and characterize the practical benefits for all the involved stakeholders. In this paper, we offer the first comprehensive attempt to analyze and understand the competition and cooperation behavior of dissimilar players within this novel ecosystem, which boils down to the following *four major contributions*.

1) **Initial market formulation.** We introduce viable strategies of the LSPs (licensed-band service providers) when operating in the new market of the aerial mmWave access systems. A vertically differentiated market is comprehensively modeled where LSPs first determine the specification of their offered services and then decide on the prices or the quantities of the services they offer according to the Bertrand or Cournot competition models. Our proposed formulation enables a valuable comparison of the equilibrium points established with the two considered initial games.
2) **Analysis of market dynamics.** We construct a novel analytical framework that captures the short-term market dynamics featuring dissimilar players, several LSPs and one USP (unlicensed-band service provider), as the latter enters the subject market. Our dynamic game theoretic methodology allows to carefully follow the cooperative interactions between the LSPs and their competition against the USP counterpart, as well as thoroughly characterize both price- and sociality-driven evolution of customer preferences when making the service provider selection. Importantly, our proposed methodology is not limited to static scenarios and can easily be extended for the cases of user mobility by incorporating more realistic air-to-ground channel modeling parameters as, e.g., those found in [41], [42].
3) **Numerical performance evaluation.** We systematically report important numerical results for the considered market players under the realistic assumptions on the mmWave channel modeling, signal propagation, and aerial access point (AAP) operation. Our findings open the door to an exciting technology innovation when AAPs belonging to different LSPs serve customers in cooperation, thus allowing multiple operators to share the access infrastructure. A detailed study of temporal evolution in market shares and resulting profits is delivered for both the Bertrand and Cournot competition models.
4) **Large-scale system-level validation.** We verify our extensive analytical results with in-depth system-level simulations that are grounded in reality and constructed after the meaningful real-world scenarios. The employed simulation platform integrates considerable knowledge behind the principles of mmWave system operation as well as employs substantiated and adequate assumptions on the AAP deployment behavior. The simulation results are made available to validate the core assumptions of our proposed analytical framework, assess the true market dynamics, and support the key practical learnings.

II. PROPOSED SYSTEM MODEL

In this section, we outline the considered system as well as introduce its main assumptions.

A. SCENARIO OF INTEREST

We focus on an open-air, densely crowded scenario (e.g., a festival or any other outdoor event) within a particular area of interest, where participants are located on the ground. The mobile devices of these people – *potentially active* in terms of wireless access – are equipped with radio transceivers and are able to operate on either *licensed* or *unlicensed* mmWave frequencies.

Assumption 1: For modeling the mmWave channel, we represent a human body as a cylinder of height h_b and diameter $2r_b$, and further assume that positions of the centers of cylinders are spatially distributed with the density of μ. We note that not all of our mass event participants may use mmWave radios and also assume a certain share of potentially active ones, termed customers. *Further, the average elevation of the mobile devices equals h_d, and the projections of the active devices on the ground are also spatially distributed with the respective density of $\mu_0 << \mu$.*

Mobile devices of customers on the ground may be served by aerial mmWave access points (or drone cells) that belong to a certain owner (i.e., service provider). These flying access nodes may be deployed temporarily within the area of interest to support very high but relatively short-term connectivity demand on the ground during the event in question.

Assumption 2: We assume that N_i AAPs (aerial access points) within a certain service provider's deployment i (termed here a fleet) are identical, uniformly placed over the area, keep the same altitude h_i, and operate over the spectrum bandwidth B_i. An AAP may serve a customer's device with a beam of half-angle ϕ (half of the aperture), which is directed at the inclination angle $\beta \leq \beta_{\max}$, where $\beta_{\max} < \pi/2$ follows from physical restrictions (i.e., the angle between the vertical and the beam cone axes cannot exceed a certain maximum).

If a certain device is associated with the fleet i based on a particular customer agreement (the agreements are all indivisible and mutually exclusive), it will be served by the

closest AAP of the corresponding fleet. Let us consider a link of the tagged device associated with the fleet i. We assume that one of the following alternative situations may take place (see, e.g., [13]):

- there is line-of-sight (LOS) propagation between the device and the corresponding AAP,
- the device is blocked by the body of its owner or another person, but there still exists a sufficiently strong path for the reflected beam,
- the device is fully blocked and thus has no usable connection to the AAP.

In order to address the above options, we introduce the following assumptions.

Assumption 3: Signal propagates according to a free-space model and hence, depending on the link between the AAP and the device, the received power at distance $d \leq h \tan \beta_{\max}$ *may assume one of the following values*:

$$\begin{cases} p_{rx} = p_{tx} G_a \dfrac{G_i}{h^2 + d^2}, & \text{if LOS exists,} \\ p_{rx} = p_{tx} G_{NLOS} G_a \dfrac{G_i}{h^2 + d^2}, & \text{if no LOS, but signal is reflected,} \\ p_{rx} = 0, & \text{if no signal at all,} \end{cases} \tag{1}$$

where p_{tx} *is the fixed transmit power,* $G_a = \frac{2}{1-\cos\phi}$ *is the antenna gain,* $G_i = \left(\frac{c}{4\pi f_i}\right)^2$ *is a path gain constant,* f *is the signal frequency,* $c = 3 \cdot 10^8$ *m/s is the speed of light. Here,* G_{NLOS} *is a constant decrease in signal power due to reflection (additional attenuation factor as in [13]), which is assumed to be fixed across the network.*

Based on the received power, we may estimate the actual throughput of the device connected to the AAP of the fleet i and located at the distance d according to the Shannon's formula:

$$T = \Delta B_i \log_2 \left(1 + \frac{p_{rx}}{N_0}\right), \tag{2}$$

where N_0 is the noise plus interference level and ΔB_i is a share of effective bandwidth available to the link in question. We assume that each device always uses the full channel bandwidth (which may vary depending on the choice of a provider), while the time is shared between all the connected devices equally (e.g., as a result of the round-robin scheduling as in [36]). Owing to the beamforming capability on the mmWave AAPs, we can analyze our scenario as noise-limited, and thus N_0 is assumed constant.

Assumption 4: In addition, we assume that the number of AAPs within each fleet is sufficient to cover the area of interest. In particular, the distance between the two AAPs is $2R_{AAP}$, $R_{AAP} \leq h \tan \beta_{\max}$. *This readily implies a lower bound on the number of AAPs (for a hexagonal grid):*

$$N_{\min} = \left\lceil \frac{R}{2h \tan \beta_{\max}} + 1 - \sqrt{2} \right\rceil \left\lceil \frac{R\sqrt{\frac{4}{3}}}{2h \tan \beta_{\max} + 1 - \sqrt{\frac{8}{3}}} \right\rceil + \left\lfloor \left\lceil \frac{R\sqrt{\frac{4}{3}}}{2h \tan \beta_{\max} + 1 - \sqrt{\frac{8}{3}}} \right\rceil \right\rfloor. \tag{3}$$

The above expression (or similar, depending on the actual deployment) is merely an example and may be obtained based on straightforward geometric reasoning; thus, we omit its derivation here to save space.

B. MAIN PLAYERS AND THEIR INTERACTIONS

In this work, we differentiate between the following *three types* of players in our system: (i) multiple customers demanding service, (ii) L LSPs (licensed-band service providers) operating in *licensed* mmWave spectrum and "supposedly" responsible for the announced QoS, and (iii) one USP (unlicensed-band service provider) operating in free-to-use *unlicensed* mmWave frequencies and aiming to offer best-effort service. The interactions of interest between these players also belong to the following *three types*:

A. A tagged customer may be served by its own LSP paying a *fixed* price $p_i, i = 1, \ldots, L$ (per unit time). For that matter, the LSP provides the customer with a mobile subscription (e.g., a SIM-card) in advance, where the choice of an LSP is made based on the individual customer preferences (see below).

B. Another alternative for the customer is to be served by the USP paying a *dynamic* price $p_0(t)$. We note that all of our devices with mmWave radios may be served by the USP, including those that do not have an LSP subscription provided in advance.

C. Finally, an LSP may request *assistance* from another LSP and utilize its infrastructure to serve a certain customer, e.g., if the latter is geometrically closer to other provider's AAP (see Fig. 2 for details). In this case, the served customer is unaware of such cooperation and continues to pay its regular price $p_i, i = 1, \ldots, L$. The LSPs may share the resulting surplus according to a certain partitioning model, e.g., using the Shapley vector [33].

C. STRATEGIES AND PAYOFFS

Below, we discuss the strategies and the corresponding payoffs of our three types of players.

1) **All LSPs** aim to support the desired QoS and keep their subscribers satisfied. To do so, one LSP may offload some of its customers (connections) to another LSP, and thus have them served on its own spectrum, but using the airtime of the assisting LSP. In such a situation, the assisting LSP's infrastructure will effectively act as a "proxy" AAP.
   Strategy of the LSP i includes offering prices p_i per unit time for its customers as well as announcing a certain QoS (e.g., throughput) at the initial stage of the market game.
2) **USP's** profit comprises the fees paid by all of its customers (potentially including former customers of either LSP and those without the LSP subscriptions).

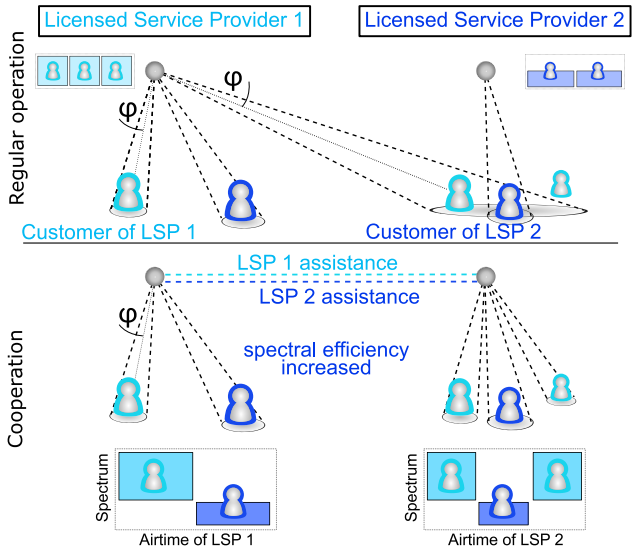

FIGURE 2. Cooperation between service providers: mutual assistance of the LSPs.

Strategy of the USP includes offering price $p_0(t)$ for providing best-effort service to its customers.

3) Each of N *active* customers aims at maximizing its utility $U(T, p)$, that is, a function of price and experienced throughput.

Strategy of a customer includes choosing a service provider (e.g., its own LSP, if applicable, or the USP). Accordingly, a customer may prefer its own LSP (in case a SIM-card has been purchased in advance) or connect to the USP instead.

D. CUSTOMER'S PREFERENCES

In contrast to most past work, we assume in this paper that customers *are not identical* in their preferences, which conveniently reflects their different financial capabilities, tastes, or priorities. We thus consider a vertically differentiated market [43], where potential customers agree on ranking diverse products (in our case, mmWave access offers) in the order of quality preference according to some utility function. However, their willingness to pay remains variable due to, e.g., budget restrictions.

Assumption 5: In our scenario, we introduce the following utility function:

$$U(\theta, T, p) = \theta \cdot s(T) - p, \tag{4}$$

where s is an increasing quality function determined by the throughput T that the customer may observe while making a decision (i.e., either announced by the provider at the initial stage or experienced during operation), p is the price per airtime, and θ is the taste parameter [29]. The latter is a typical measure of the buyer's preference in the differentiated markets. The higher its taste parameter is, the more a customer is willing to pay for a better quality service. Generally, zero utility value corresponds to not buying the product, and thus if $U(\theta, T, p) \leq 0$, then a customer would decide to refrain from purchasing the mmWave access service. We assume that θ is distributed within the interval $[0, \theta_{\max}]$ according to a certain probability density $h_\theta(\theta)$.

Our customers are *rational*, that is, they always make decisions targeting the better utility value. Here, zero utility corresponds to the situation when a customer decides not to connect, while zero lower bound on θ implies that there always exists someone who decides not to connect at all (i.e., we assume that our setup is not "covered market" in order to be able to apply the Cournot competition model further on).

III. INITIAL STAGE OF OUR GAME FORMULATION

A. GENERAL REMARKS

We decompose our subsequent modeling into two consecutive parts, which are the (i) *initial-stage* game formulation where LSPs divide the market in advance and (ii) *dynamic* game development after the USP enters the market in equilibrium.

1) INITIAL STAGE

At the initial, *long-term* stage, only major players (the LSPs 1,..., L) are participating in a differentiated market game with *two phases*: first, deciding on the maximum quality level to attract customers and second, competing in price or, alternatively, in quantity. We consider both price and quantity competitions as they lead to different equilibrium points, and there is still no consensus in current literature as to which type of competition is preferred. At the point of equilibrium, a certain share $D_1 \in (0, 1)$ of customers have purchased subscriptions (SIM-cards) of the LSP 1, while $D_i \in (0, 1 - \sum_{j=1}^{i-1} D_j)$ have acquired SIM-cards of the LSP i. The remaining customers may be not connected to either LSP, since our setting is not a "covered market". We briefly summarize the above as:

- **Players**: L LSPs.
- **Strategies**: first – qualities, then – prices/quantities.
- **Payoff**: utility of each LSP (subscriber payments minus costs).

2) DYNAMIC STAGE

At the second, *short-term* stage, a new market player (the USP) is intruding the system where the LSPs operate at the equilibrium point. The USP announces its dynamic price $p_0(t)$ at time moment t. Based on their utility function, customers of the LSP i may decide to prefer the USP, while previously non-participating customers (having share $y_0 \in [0, 1 - \sum_{j=1}^{L} D_j]$) may connect *only* to the USP. Our system tracks the shares x_i, y_0, and y_i, where x_i correspond to customers currently utilizing service of the LSP i, and y_i, $i = 1, \ldots, L$ denotes those who change their LSP i for the USP.

We assume that every customer of the LSP i is aware of both prices $p_0(t)$ and p_i as well as knows its current throughput ($T_0(t)$ or $T_i(t)$). Further, customers are able to interact with each other (owing to their close proximity within the area of interest) and hence may *imitate* strategies of others (see,

e.g., [39]). In our scenario, a customer of the LSP i or USP with the taste θ decides to inquire another customer from the potential group of the USP or LSP j about the experienced service quality. Based on the received information T_j, the tagged customer calculates its own potential utility $U(\theta; s(T_j), p_j)$ and, if the potential service is better than the current one, changes its service provider with the probability that is proportional to the difference $U(\theta; s(T_j), p_j) - U(\theta; s(T_i), p_i)$.

Summarizing, the considered dynamic game may be described by:

- **Players**: USP and the customers.
- **Strategies**: $p_0(t)$ for the USP and service provider selection for the customers.
- **Population state**: shares of the customers $(y_0, y_1, \ldots, y_L)$.
- **Payoff**: utility of the USP (pure profit) and utility of the customers.

The overall structure of the dynamic game for $L = 2$ is illustrated in Fig. 3.

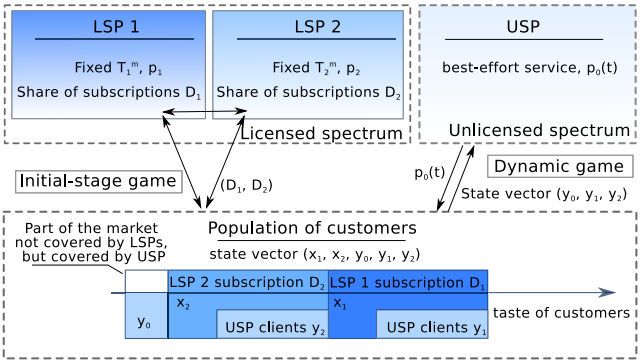

FIGURE 3. Interactions in the considered dynamic game for $L = 2$.

B. PROFITS OF THE LSPs AT THE INITIAL STAGE

First, L LSPs play a two-stage game to divide the market and set the optimal quantity or price (here, we do not consider the market entry stage [44] for the LSPs). For the sake of further comparison, we model *both alternatives*: price setting and quantity setting types of competition, which are known in the literature as Bertrand and Cournot competition models, correspondingly. In this work, we analyze both game types in order to reveal the dependence of the results on the optimal choice of LSP strategies, namely, whether LSPs eventually offer a homogeneous product (as shown by the Cournot model) or differentiated products (as illustrated by the Bertrand model). Since both situations may happen in the real market, one model cannot be preferred over another.

At the **first** stage, all LSPs select the offered level of *quality*. We recall that quality is characterized by a data rate package with *provisionally announced maximum throughput* T_i^m, $i = 1, \ldots, L$, and the LSPs are aware of each other but make their decisions sequentially. At the **second**, competitive stage, in the Bertrand game, the LSPs decide on the *prices* $p_i, i = 1, \ldots, L$ that will be announced to the customers purchasing their SIM-cards (a mutually exclusive choice is assumed here). In contrast to that, in the Cournot game, the LSPs decide on *quantity*, which in our scenario translates into the number of subscribed customers or, equivalently, sold SIM-cards.

Making its decisions at both stages, an LSP aims to maximize its **profit**. The LSP income is determined by the financial flow from the previously subscribed and presently served customers, but to define the rest of the profit function we need to clarify the structure of the costs. The advertised service quality may not be matching the real quality, which uninformed customers face after purchasing the product. However, in our scenario, maintaining subscription (loyalty) to a particular LSP in the long run is equivalent to a "repeat purchase". Therefore, sellers are highly motivated in keeping their subscribed customers satisfied, as inspired by the theory of advertising in [45], [46]. To reflect this motivation analytically, we introduce the following assumption responsible for handling the costs of the LSPs.

Assumption 6: We assume linear costs *of improvement in the claimed quality* s_i per user, *so that an LSP would be ready to support it for its served customers. Hence, the total costs depend both on the number of served devices and the announced* T_i^m. *The latter reflects the initial investments into a fixed-term spectrum lease and/or the amounts of spectrum that could be resold (as, e.g., in [47] or [25]) or, otherwise, rented.*

In fact, the dependence of costs on the required throughput is not linear, because in practice not all of the customers are active simultaneously and the resources of the LSPs are carefully provisioned. However, for the sake of tractability of further analysis, we assume that the profit function is given by:

$$\Pi_i(\mathbf{s}, \mathbf{p}) = D_i(\mathbf{s}, \mathbf{p})\,(p_i - \nu s_i)\,, \tag{5}$$

where $D_i(\mathbf{s}, \mathbf{p})$ is a demand for the LSP i, and ν is a "quality cost coefficient". The latter may be roughly estimated from the value of the spectrum license costs to support the announced QoS normalized by the time and the total number of customers in the country of interest.

C. DEMANDS FOR THE LSPs AT THE INITIAL STAGE

To establish the Nash equilibrium of our game at its initial stage, we exploit the principle of *backward induction*. Assuming that the levels of quality $s_i = s(T_i^m)$ (or, equivalently, the levels of the announced throughput T_i^m) are fixed, we first obtain the equilibrium for the Bertrand price game and the Cournot quantity game. Without loss of generality, we may assume that $s_i \geq s_{i+1}$ ($T_i^m \geq T_{i+1}^m$), and hence $p_i \geq p_{i+1}$, since the sellers are targeting the rational customers, and we consider *one-dimensional* product differentiation (otherwise, (4) would contain additional components related to other criteria [48]). Moreover, since the function $\frac{p(s)}{s}$ is monotonically decreasing, the inequality $\frac{p_i}{s_i} > \frac{p_{i+1}}{s_{i+1}}$ holds for any $s_i \neq s_{i+1}$ and as a result, $\frac{p_i - p_{i+1}}{s_i - s_{i+1}} < \frac{p_{i-1} - p_i}{s_{i-1} - s_i}$ and $\frac{p_L}{s_L} < \frac{p_{L-1} - p_L}{s_{L-1} - s_L}$ (both inequalities can be easily proved).

Following [29], and based on the fixed price and quality levels, we determine the following points of indifference for a tagged customer:

- point of indifference to buying or not buying the service of the most affordable LSP L is denoted by the parameter $\theta_{\varnothing,L} = \frac{p_L}{s_L}$ (follows from $U(\theta, s_L, p_L) = 0$),
- point of indifference to buying the service of the LSP $i+1$ or the LSP i corresponds to the parameter $\theta_{i+1,i} = \frac{p_i - p_{i+1}}{s_i - s_{i+1}}$ (follows from $U(\theta, s_i, p_i) = U(\theta, s_{i+1}, p_{i+1})$).

Therefore, for $\theta_{\varnothing,L} < \theta_{L,L-1} < \ldots < \theta_{i+1,i} < \ldots < \theta_{\max}$ the corresponding demands may be rewritten as:

$$\begin{aligned} D_1(\mathbf{s};\mathbf{p}) &= \int_{\theta_{i+1,i}}^{\theta_{\max}} h(\theta)d\theta = H(\theta_{\max}) - H(\theta_{i+1,i}),\\ D_i(\mathbf{s};\mathbf{p}) &= \int_{\theta_{i,i-1}}^{\theta_{i+1,i}} h(\theta)d\theta = H(\theta_{i+1,i}) - H(\theta_{i,i-1}),\\ &\ldots,\\ D_L(\mathbf{s};\mathbf{p}) &= \int_{\theta_{\varnothing,L}}^{\theta_{L,L-1}} h(\theta)d\theta = H(\theta_{L,L-1}) - H(\theta_{\varnothing,L}), \end{aligned} \quad (6)$$

where $h(\theta)$ and $H(\theta)$ are the PDF and the CDF of the taste parameter θ, respectively. We emphasize that the shape of $h(\theta)$ has a significant effect on the solution of the considered problem. Studying a particular distribution constitutes a *standalone problem*, and therefore, for the sake of clarity we introduce the following assumption.

Assumption 7: For the purposes of illustration in this paper, we only consider a uniform distribution of the taste parameter $h(\theta) = \frac{1}{\theta_{\max}}$, $\theta \in [0, \theta_{\max}]$. In case of more than one player in the market, if $h(\theta)$ is not uniform, we may experience multiple symmetric equilibria [44], which could be investigated separately and may thus generalize the results of this work in subsequent studies.

Accordingly, the expression (7) may be then rewritten as follows:

$$\begin{aligned} D_1(\mathbf{s};\mathbf{p}) &= \frac{1}{\theta_{\max}}\left(\theta_{\max} - \frac{p_i - p_{i+1}}{s_i - s_{i+1}}\right),\\ D_i(\mathbf{s};\mathbf{p}) &= \frac{1}{\theta_{\max}}\left(\frac{p_{i-1} - p_i}{s_{i-1} - s_i} - \frac{p_i - p_{i+1}}{s_i - s_{i+1}}\right),\\ &\ldots,\\ D_L(\mathbf{s};\mathbf{p}) &= \frac{1}{\theta_{\max}}\left(\frac{p_{L-1} - p_L}{s_{L-1} - s_L} - \frac{p_L}{s_L}\right). \end{aligned} \quad (7)$$

Interestingly, despite the fact that the resulting solution depends on $h(\theta)$, the main trade-off and qualitative conclusions for the Bertrand and Cournot games would not drastically change (e.g., see [49], where the uniform distribution is compared to the triangle-shaped distribution for the case $L = 2$). In what follows, we consider the Bertrand price competition and the Cournot quantity competition models separately.

D. BERTRAND PRICE COMPETITION

In the Bertrand game, the LSPs choose prices p_i in order to maximize their profits $\Pi_i = D_i(p_i - \nu s_i)$ for the selected quality function values s_i.

Differentiating Π_i over p_i, one may calculate the optimal prices (can be verified for $L = 2$ by [49] and for $L = 2$, $\nu = 0$ by [29]) for the fixed levels of quality and $s_i \neq s_j, \forall i \neq j$ based on the following:

$$\begin{cases} \frac{\partial \Pi_1}{\partial p_1} = \left(\left(\theta_{\max} - \frac{p_1 - p_2}{s_1 - s_2}\right)(p_1 - \nu s_1)\right)'_{p_1},\\ \ldots\\ \frac{\partial \Pi_i}{\partial p_i} = \left(\left(\frac{p_{i-1} - p_i}{s_{i-1} - s_i} - \frac{p_i - p_{i+1}}{s_i - s_{i+1}}\right)(p_i - \nu s_i)\right)'_{p_i},\\ \ldots\\ \frac{\partial \Pi_L}{\partial p_L} = \left(\left(\frac{p_{L-1} - p_L}{s_{L-1} - s_L} - \frac{p_L}{s_L}\right)(p_L - \nu s_L)\right)'_{p_L}, \end{cases} \quad (8)$$

or, equivalently, from the system of linear equations w.r.t. p_i:

$$\begin{cases} 2p_1 - p_2 = \theta_{\max}(s_1 - s_2) + \nu s_1,\\ -p_1(s_2 - s_3) + 2p_2(s_1 - s_3)\\ -p_3(s_1 - s_2) = \nu s_2(s_1 - s_3),\\ \ldots\\ -p_{i-1}(s_i - s_{i+1}) + 2p_i(s_{i-1} - s_{i+1})\\ -p_{i+1}(s_{i-1} - s_i) = \nu s_i(s_{i-1} - s_{i+1}),\\ \ldots\\ -p_{L-1}s_L + 2p_L \cdot s_{L-1} = \nu s_L s_{L-1}. \end{cases}$$

For the fixed L, the resulting vector $(p_1^*(\mathbf{s}), \ldots, p_L^*(\mathbf{s}))$ should be substituted into the system $\frac{\partial \Pi_i}{\partial s_i}(\mathbf{s};\mathbf{p}) = 0, i = 1, \ldots, L$, which results in the following:

$$\begin{cases} \frac{\partial \Pi_1}{\partial s_1} = \left(\left(\theta_{\max} - \frac{p_1^*(\mathbf{s}) - p_2^*(\mathbf{s})}{s_1 - s_2}\right)\left(p_1^*(\mathbf{s}) - \nu s_1\right)\right)'_{s_1},\\ \ldots\\ \frac{\partial \Pi_i}{\partial s_i} = \left(\left(\frac{p_{i-1}^*(\mathbf{s}) - p_i^*(\mathbf{s})}{s_{i-1} - s_i} - \frac{p_i^*(\mathbf{s}) - p_{i+1}^*(\mathbf{s})}{s_i - s_{i+1}}\right)\left(p_i^*(\mathbf{s}) - \nu s_i\right)\right)'_{s_i},\\ \ldots\\ \frac{\partial \Pi_L}{\partial s_L} = \left(\left(\frac{p_{L-1}^*(\mathbf{s}) - p_L^*(\mathbf{s})}{s_{L-1} - s_L} - \frac{p_L^*(\mathbf{s})}{s_L}\right)\left(p_L^*(\mathbf{s}) - \nu s_L\right)\right)'_{s_L}. \end{cases} \quad (9)$$

Solution for the equations $\frac{\partial \Pi_i}{\partial s_i} = 0$ may be easily found, e.g., for $L = 2$. For larger numbers, one may solve the system using symbolic operations in any appropriate mathematical tool provided the condition $s_1 > s_2 > s_3$. Importantly, $\frac{\partial \Pi_1}{\partial s_1} = 0$ does not have a solution so that $s_1 > s_2 > s_3$ holds, but due to the fact that $\frac{\partial \Pi_1}{\partial s_1} > 0$, we may conclude that the maximum is located at the border, i.e., $s_1 = s_{\max}$, where $s_{\max}$ is the highest quality that the first deciding LSP may choose.

The detailed derivations for the case $L = 2$ (see Table 1 for the final expressions) are given in [49]; however, below we

shortly reformulate the main conclusions regarding the Nash equilibrium.

Proposition 1: For $L = 2$, the solution of the system (9) is a unique Nash equilibrium for the considered Bertrand game.

Proof: The proof is based on demonstrating that the following holds:

$$\begin{aligned} &\Pi_i(s_1^*, s_2^*) \geq \Pi_i(s_1, s_2^*), \quad \text{for any } s_1 < s_1^*, \\ &\text{and } \Pi_i(s_1^*, s_2^*) \geq \Pi_i(s_1^*, s_2), \quad \text{for any } s_2 \neq s_2^*, \end{aligned} \tag{10}$$

which may be verified using the first and the second derivatives of the profit function. □

For cases $L > 2$, the system does not have a solution so that $s_1 > s_2 > s_3$ and, therefore, the Nash equilibrium does not exist for the considered Bertrand game (as well as for some other similar formulations). The formal proof of this fact constitutes a standalone problem, which we intentionally keep out of the scope of this paper.

E. COURNOT QUALITY COMPETITION

While in case of the Bertrand market the LSP i controls the price p_i so that the share of users is naturally derived through the demand function, in the Cournot market the LSPs control the quantity of customers (in particular, the number of users in our scenario) and, hence, the prices are determined based on the following inverted system of demand functions:

$$\begin{cases} p_1(\mathbf{s}, \mathbf{D}) = \theta_{\max}(s_1 - \sum_{k=1}^{L} D_k s_k), \\ \dots \\ p_i(\mathbf{s}, \mathbf{D}) = \theta_{\max}(s_i - s_i \sum_{k=1}^{i-1} D_k - \sum_{k=i}^{L} D_k s_k), \\ \dots \\ p_L(\mathbf{s}, \mathbf{D}) = \theta_{\max}(s_L - s_L \sum_{k=1}^{L} D_k), \end{cases} \tag{11}$$

which may be obtained from the expressions (7) by the mathematical induction. Moreover, as we will need the corresponding partial derivative below, we may immediately calculate $\partial p_i / \partial D_i = -\theta_{\max} s_i$.

We further produce the quantity response functions maximizing the profit for the fixed qualities s_i by substituting the demand functions (11) into the expression for the LSP profit $\Pi_i = D_i(p_i - \nu s_i)$ and calculating the respective derivatives $\partial \Pi_i / \partial D_i = p_i(D_i) - \nu s_i + D_i \cdot \partial p_i / \partial D_i$:

$$\begin{cases} \frac{\partial \Pi_1}{\partial D_1} = \theta_{\max}(s_1 - \sum_{k=1}^{L} D_k s_k) - \nu s_1 - D_1 \cdot \theta_{\max} s_1, \\ \dots \\ \frac{\partial \Pi_i}{\partial D_i} = \theta_{\max}(s_i - s_i \sum_{k=1}^{i-1} D_k - \sum_{k=i}^{L} D_k s_k) - \nu s_i - D_i \cdot \theta_{\max} s_i, \\ \dots \\ \frac{\partial \Pi_L}{\partial D_L} = \theta_{\max}(s_L - s_L \sum_{k=1}^{L} D_k) - \nu s_L - D_L \cdot \theta_{\max} s_L. \end{cases}$$

The sought demand functions $D_i^*(\mathbf{s})$ that maximizes the LSP profit may be symbolically obtained from the system of L linear equations $\frac{\partial \Pi_i}{\partial D_i} = 0, i = 1, .., L$.

Substituting these optimal $D_i^*(\mathbf{s})$ demand functions into (11), we establish the prices $p_i(\mathbf{s})$ set by the LSPs and, thus, the corresponding profit $\Pi_i(\mathbf{s})$ as a function of quality $\mathbf{s}$.

In the second stage of backward induction, we attempt to derive the optimal level of qualities that maximize the profit $\Pi_i(\mathbf{s})$ by finding solutions of the equations $\frac{\partial \Pi_i}{\partial s_i} = 0, i = 1, .., L$ separately (we remind that the LSPs select s_i sequentially, not simultaneously).

Similar to the case of Bertrand game, the solution of this system may be easily derived for $L = 2$. Particularly, denoting s_1/s_2 as x, we conclude that there exists no solution $x > 1$ for any of the equations $\frac{\partial \Pi_i}{\partial s_i} = 0$. Since both $\frac{\partial \Pi_1(s_1, s_2)}{\partial s_1}$ and $\frac{\partial \Pi_2(s_1, s_2)}{\partial s_2} > 0$, the point of maximum is located at the right border of the interval for s, that is, $s_1^* = s_{\max}$ and $s_2^* = s_{\max}$, where $s_{\max}$ is the maximum level that an LSP can choose. The final prices, profits, as well as points of indifference for $L = 2$ are summarized in Table 1. For larger numbers, one may search for a solution symbolically given the condition $s_1 > s_2 > s_3$, and the maximum is also located at the border, $s_1 = s_{\max}$.

TABLE 1. Comparing our initial game solutions for $L = 20$ [49].

Game type	Bertrand	Cournot
Quality of LSP 1[A]	s	s
Quality of LSP 2	$0.5714s$	s
Point $\theta_{\varnothing,2}$	$0.8750\nu + 0.125\theta$	$0.6667\nu + 0.3333\theta$
Point $\theta_{1,2}$	$0.5833\nu + 0.4167\theta$	$0.6667\nu + 0.3333\theta$
Profit of LSP 1	$0.1458s\frac{(\theta-\nu)^2}{\theta}$	$0.1111s\frac{(\theta-\nu)^2}{\theta}$
Profit of LSP 2	$0.0208s\frac{(\theta-\nu)(\theta-7.0\nu)}{\theta}$	$0.1111s\frac{(\theta-\nu)^2}{\theta}$
Aggregate MP[B]	$0.1667s\frac{(7\nu^2+4\theta^2-11\nu\theta)}{4\theta}$	$0.2222s\frac{(\theta-\nu)^2}{\theta}$
Price of LSP 1	$0.2500s(3\nu + \theta)$	$0.3333s(2\nu + \theta)$
Price of LSP 2	$0.0714s(7\nu + \theta)$	$0.3333s(2\nu + \theta)$
Costs of LSP 1	$0.5833\nu s\frac{(\theta-\nu)}{\theta}$	$0.3333\nu s\frac{(\theta-\nu)}{\theta}$
Costs of LSP 2	$0.1667\nu s\frac{(\theta-\nu)}{\theta}$	$0.3333\nu s\frac{(\theta-\nu)}{\theta}$
Demand of LSP 1	$0.5833\frac{(\theta-\nu)}{\theta}$	$0.3333\frac{(\theta-\nu)}{\theta}$
Demand of LSP 2	$0.2917\frac{(\theta-\nu)}{\theta}$	$0.3333\frac{(\theta-\nu)}{\theta}$
Total demand	$0.8750\frac{(\theta-\nu)}{\theta}$	$0.6667\frac{(\theta-\nu)}{\theta}$

[A] For brevity, $\theta = \theta_{\max}$, $s = s_{\max}$.
[B] Market profit.

Proposition 2: For $L = 2$, the obtained solution for the Cournot game is a unique Nash equilibrium.

Proof: Follows from a verification of the same conditions as for the Bertrand game. □

For $L > 2$, the Nash equilibrium does not exist, and we keep the rigorous proof of this fact out of the scope of this paper.

As a result of all the above derivations, we obtain the *divided* (albeit not covered) market at time moment $t = 0$, which is illustrated in Fig. 4. In the figure, the upper part corresponds to our static initial solution.

IV. DYNAMIC DEVELOPMENT OF GAME FORMULATION

In this section, we introduce a new player on the market, namely, the USP. In our scenario, the USP enters the market where the LSPs are operating in equilibrium for a *short-term*

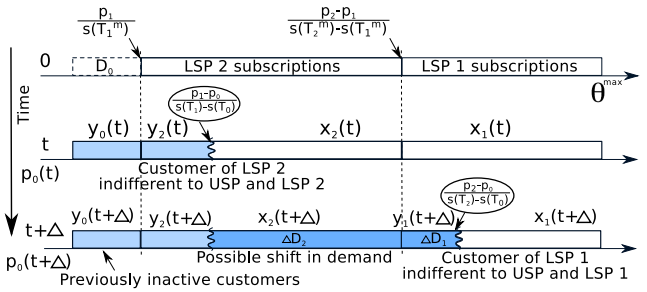

FIGURE 4. Illustration of our vertically differentiated market for $L = 2$.

period, thus distorting the balance. For the sake of clarity, below we provide all of our derivations for $L = 2$. However, the subsequent expressions may be trivially extended to the case of more participants.

Assessing the changes in the customer alignment picture constitutes the theoretical target of this section. We note that in the considered market the customers are differentiated by their experienced spectral efficiency (due to the actual geometry of their locations) and their preferences to the price/throughput trade-off (according to our assumption of a vertically differentiated market). To tackle the resulting complex and multidimensional problem, we capture the system dynamics by averaging the spectral efficiencies across the coverage areas of the AAPs, which may be equivalent to characterizing customer mobility.

A. DYNAMIC SETUP AND mmWave PROPERTIES

In order to follow the dynamic evolution of customer utility, we first focus on deriving the average spectral efficiency, which is a function of the number of simultaneously served customers per mmWave AAP. For that matter, we consider a *tagged* AAP of the fleet i representing the average system behavior within this fleet. Owing to the flexibility of drone cell deployment as well as minding our earlier assumption of uniform AAP placement, we further assume that the coverage area of this AAP may be approximated by a circle of radius R_{AAP} that is equal to a half of the distance between two neighboring AAPs (as per Assumption 4):

$$R_{AAP} = \frac{R}{\sqrt{2} + \left\lceil \frac{R}{2h_i \tan \beta_{\max}} + 1 - \sqrt{2} \right\rceil - 1}. \tag{12}$$

We note that the above has been derived by analogy to (3) reflecting a particular considered deployment, and is meant here to illustrate the radius estimation.

Assumption 8: Specifically, we assume that user devices are distributed according to a Poisson Point Process (PPP) with the density μ_0, which has been introduced earlier in Assumption 1.

Then, the number of devices per AAP may be calculated as:

$$n_i = \mu_0 \pi R_{\text{AAP}}^2 x_i, \quad i = 1, 2, \; n_0 = \mu_0 \pi R_{\text{AAP}}^2 (y_0 + y_1 + y_2), \tag{13}$$

where x_i, $i = 1, 2$ correspond to the shares of customers for the LSPs and y_i, $i = 0, 1, 2$ is the total share of customers for the USP.

Assumption 9: For the sake of analytical tractability, we replace random spectral efficiencies of the customers with a spectral efficiency value averaged across the coverage area of the tagged AAP.

Due to our PPP assumption, the distribution of distances d to the AAP within a circle of radius R_{AAP} equals $f_d(x) = \frac{2x}{R_{\text{AAP}}^2}$. Therefore, the average spectral efficiency $\overline{\eta}(R_{\text{AAP}})$ may be established by calculating the following integral:

$$\overline{\eta}(R_{\text{AAP}}) = \int_0^{R_{\text{AAP}}} \log_2 \left(1 + \tilde{p}(q_{\text{LOS}} + q_{\text{NLOS}} G_{\text{NLOS}})\right) \frac{2x}{R_{\text{AAP}}^2} dx, \tag{14}$$

where $\tilde{p} = p_{tx} \frac{G_i G_a}{(h^2 + d^2) N_0}$ for brevity, G_i is the path gain defined in Assumption 3, G_a is the antenna gain, and the probabilities of LOS/NLOS link have different nature by contrast to the conventional approach in [50]. These are derived in Appendix and summarized here as:

$$\begin{cases} q_{\text{LOS}}(d) = e^{-\mu d \cdot 2 r_b \left(\frac{h_b - h_d}{h - h_d}\right)}, & \text{if LOS exists,} \\ q_{\text{NLOS|no LOS}}(d) = \left(1 - \exp\left(-\mu \dfrac{\pi \, (h \tan(\phi))^2 \cdot \cos(\phi)}{\sqrt{\cos^2(\phi) - \frac{d^2}{d^2 + h^2}}}\right)\right) \\ \quad \times \left(1 - q_{\text{LOS}}(d)\right), & \text{if no LOS (NLOS exists).} \end{cases} \tag{15}$$

The *closed-form* approximation is based on the fact that $E[f(x)] \approx f(E[x])$ and is given by:

$$\overline{\eta}(R_{\text{AAP}}) = \log_2 \left(1 + p_{tx} \frac{G_i G_a (q_{\text{LOS}} + q_{\text{NLOS}} G_{\text{NLOS}})}{\left(h^2 + \left(\frac{2}{3 R_{\text{AAP}}}\right)^2\right) N_0}\right), \tag{16}$$

where the above numerical solution remains suitable for the necessary further calculations. To assist in the process, Fig. 5 illustrates the changes in the slope of spectral efficiency as averaged over a circle of varied radius for 28 and 60 GHz. It clearly indicates the impact of blockage at lower AAP altitudes as well as shows the maximum distance to the receiver.

B. USP MARKET ENTRY

In our formulation, the population state may be described by the vector (y_1, y_2, y_0), which denotes the shares of customers connected to the USP having purchased a SIM-card of the LSP 1 and the LSP 2, correspondingly, or having no SIM-card at all. Further, the shares of the customers actively using the service by the LSPs may be derived directly from the initial-stage demand $x_1(t) = D_1^* - y_1(t)$, $x_2 = D_2^* - y_1(t)$ (we remind that the customers are not allowed to change their SIM-cards during our dynamic short-term game).

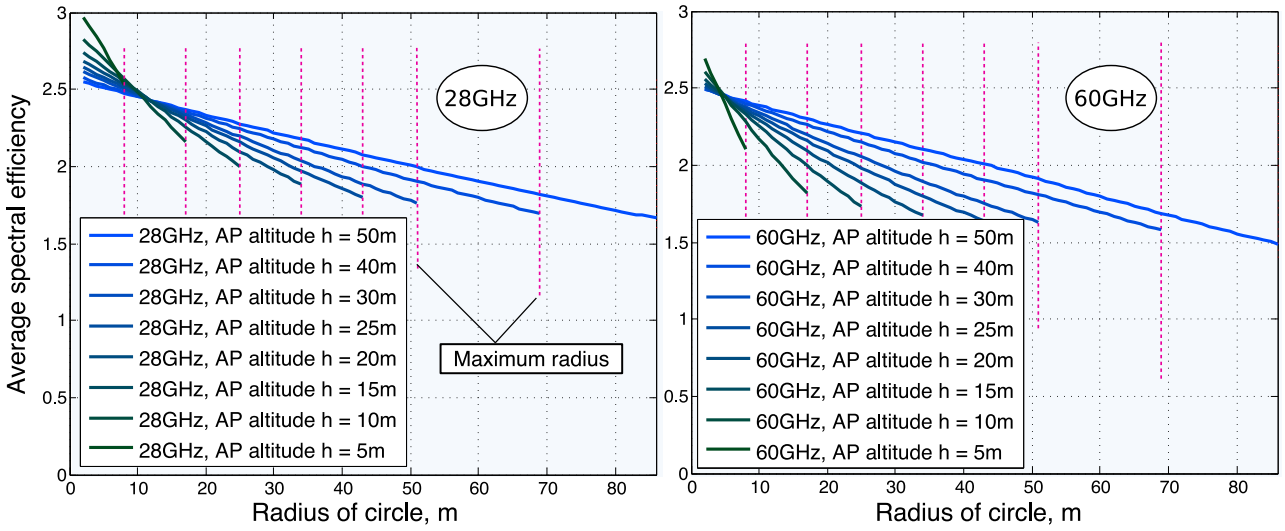

FIGURE 5. Spectral efficiency averaged over a circle of varied radius.

Given the information on $(y_0(t), y_1(t), y_2(t))$, the USP attempts to make its optimal decision on the dynamic price $p_0(t)$ that maximizes its total profit (in the absence of full market information), which in turn directly depends on both the number of connected customers and the price itself. For the fixed price p_0 and the estimated average actual throughput $\frac{B_{SP}\eta_{SP}}{y_1+y_2+y_0}$ per customer, we may establish the USP profit as:

$$\Pi_0 = p_0(t)D_0(t) = p_0(t)\left(y_0(t) + y_1(t) + y_2(t)\right), \quad (17)$$

where y_0 denotes the proportion of the customers coming from a previously inactive share of the market (those who did not purchase any SIM-card before).

Further, let the USP be unaware of future customer behavior and our hidden customer reaction functions, so that the USP could not maximize (17) explicitly. Then, its *heuristic choice* would be to react flexibly to the changes in customer demand. In particular, if the number of subscribers decreases, then the USP lowers the price and vice versa. Therefore, the stationary point for price $p(t)$ is defined by the constant demand of the USP:

$$\frac{d(y_0(t) + y_1(t) + y_2(t))}{dt} = 0. \quad (18)$$

Further, we assume that the considered price dynamics set by the USP satisfies the following equation:

$$\frac{dp}{pdt} = c_{\text{price}} \frac{d(y_0(t) + y_1(t) + y_2(t))}{dt}, \quad (19)$$

that is, the relative increment of the USP price is proportional to the increment in the number of currently served customers. We note that the latter is adopted as one of the reasonable examples where the USP acts rationally, and other USP strategies may in principle be considered.

C. DECISIONS OF CUSTOMERS

In order to mimic customer decisions when there is a choice between two utility values, we introduce the following assumption:

Assumption 10: We assume that if there is a utility difference of $\Delta U(\theta)$ between its possible value and the current one, the customer decides to change or imitate the strategy with the probability:

$$p_u\left(\Delta U(\theta)\right) = \frac{2}{1 + e^{-c_u \Delta U(\theta)}} - 1, \quad \text{for } \Delta U(\theta) > 0. \quad (20)$$

The above consideration tightly approximates the behavior of customers with arbitrary levels of patience, as given by the "impatience" coefficient c_u. In particular, $p_u(0) = 0$ (no changes whatsoever) and $p_u(\Delta U \to \infty) = 1$. This logistic function is a convenient formulation to reflect the decision making probability in the absence of information on the actual range of utility values within our game.

Modeling customer behavior in more detail, we employ a notion of proximity-based social interaction. Accordingly, the customers do not know the actual quality of services they had never used before, but they may "talk" to other customers with a certain degree of γ (could be regarded as a proximity-based interaction possibility). It effectively means that at some point of time the tagged customer may select another customer from the alternative service group to inquire for its service quality. When the USP announces the price $p_0(t)$ at the state (y_0, y_1, y_2), there could be three types of *mutually exclusive* reactions of the LSP customers as follows.

1) **Gossiping.** At the moment $t + \Delta t$, a customer of the LSP i decides to assess its quality and thus inquires someone connected to the USP, if any, with the probability γ. Knowing the alternative quality $s(T_0)$ at time t, said customer may decide to change its current service

provider, if $U(\theta; s(T_0), p_0) > U_i(\theta; s(T_i), p_i)$ with the probability $p_u(\Delta U(\theta))$. The corresponding probability is defined as:

$$\xi\gamma(y_0 + y_1 + y_2)p_u\left(U(\theta; s_0, p_0) - U(\theta; s_i, p_i)\right), \tag{21}$$

where $s_i = s(T_i)$ for brevity.

2) **Curiosity.** Another alternative is to connect to the USP out of "human curiosity", which is here independent of either social opinion or own quality observation, but dictated by human nature to explore new opportunities. We note that our earlier assumption on the rationality of the customers still holds here, since curiosity aims solely at improving the utility. For the "curiosity" factor α, the corresponding probability is given by:

$$\xi(1-\gamma)\alpha_c. \tag{22}$$

3) **Dissatisfaction.** The last considered type of user reactions is when the customer is highly dissatisfied with the current service – which, e.g., happened to be far worse than what was expected – and decides to connect to the USP with the probability comprising the "dissatisfaction" factor δ that corresponds to the actual level of disappointment, which leads us to:

$$\xi(1-\gamma)(1-\alpha_c)\delta p_u\left(U(\theta; s(T_i^m), p_i) - U(\theta; s_i, p_i)\right). \tag{23}$$

We note that the probability ξ to consider changing the current service provider is but a technical parameter here, which regulates the rate of the process in question as well as determines how frequently the USP price is reconsidered. The parameters α, γ, and δ are assumed fixed for all of the customers. Furthermore, for backward transitions from the USP to the LSP service, the above three options hold as well:

1) **Gossiping.** For a customer already connected to the USP, the "gossiping rate" toward its initial subscription is estimated as:

$$\xi\gamma \cdot x_i p_u\left(U(\theta; s_i, p_i) - U(\theta; s_0, p_0)\right). \tag{24}$$

2) **Curiosity.** The "curiosity rate" remains the same as in (22).

3) **Dissatisfaction.** The corresponding probability based on the level of dissatisfaction is given by:

$$\xi(1-\gamma)(1-\alpha_c)\delta p_u\left(U(\theta; s(T_i^m), p_i) - U(\theta; s_0, p_0)\right), \tag{25}$$

where T_i^m is the announced throughput and $s(T_i^m)$ is the solution to the initial-stage game of the LSPs.

We note that previously inactive customers do not have expectations and thus may select the USP at the moment t. Hence, they do so if, after they inquire for the relevant information, the new utility value is above zero, that is, with the probability $\xi\gamma p_u(U(\theta; s_0, p_0))$, or out of curiosity $\xi(1-\gamma)\alpha$, since they do not expect any QoS guarantees. Also, these users disconnect from service with the probability $\xi p_u\left(-U(\theta; s_0, p_0)\right)$, if at a certain time moment their utility drops below zero.

D. CAPTURING SYSTEM DYNAMICS

In order to capture the dynamic evolution of both the **customer** and the **USP** strategies, we further model the behavior of the customers on the market independently of their personal preferences θ, by averaging across the corresponding market shares. Even though within one group the customers still tend to act non-uniformly, this approximation appears to be surprisingly accurate (as we confirm with simulations later on) to model the overall market evolution. First, we derive all the needed expressions for describing said dynamics and then separately calculate the corresponding coefficients (i.e., rates $Q^{\mathrm{X}}_{i\to j}$, see below).

We continue by constructing a system of differential equations, according to which our market is evolving with time:

$$\begin{cases}
\frac{dy_1}{dt} = (D_1 - y_1)\xi\gamma(y_0+y_1+y_2)\cdot Q^{\mathrm{G}}_{1\to 0} & \text{// gossiping}\\
+(D_1 - y_1)\xi\alpha_c(1-\gamma) & \text{// curiosity}\\
+(D_1 - y_1)\xi\delta(1-\gamma)\cdot Q^{\mathrm{D}}_{1\to 0} & \text{// dissatisfaction}\\
-y_1\xi\gamma(D_1 - y_1)\cdot Q^{\mathrm{G}}_{0\to 1} & \text{// gossiping}\\
-y_1\xi\alpha_c(1-\gamma) & \text{// curiosity}\\
-y_1\xi\delta(1-\gamma)\cdot Q^{\mathrm{D}}_{0\to 1}, & \text{// dissatisfaction}\\
\frac{dy_2}{dt} = (D_2 - y_2)\xi\gamma(y_0+y_1+y_2)Q^{\mathrm{G}}_{20} & \text{// gossiping}\\
+(D_2 - y_2)\xi\alpha_c(1-\gamma) & \text{// curiosity}\\
+(D_2 - y_2)\xi\delta(1-\gamma)\cdot Q^{\mathrm{D}}_{2\to 0} & \text{// dissatisfaction}\\
-y_2\xi\gamma(D_2 - y_2)\cdot Q^{\mathrm{G}}_{02} & \text{// gossiping}\\
-y_2\xi\alpha_c(1-\gamma) & \text{// curiosity}\\
-y_2\xi\delta(1-\gamma)\cdot Q^{\mathrm{D}}_{0\to 2}, & \text{// dissatisfaction}\\
\frac{dy_0}{dt} = (D_0 - y_0)\xi\gamma(y_0+y_1+y_2)\cdot Q_{\varnothing\to 0} & \text{// gossiping}\\
+(D_0 - y_0)\xi\alpha_c(1-\gamma) & \text{// curiosity}\\
-y_0\xi\cdot Q_{0\to\varnothing}, & \text{// low utility}\\
\frac{dp_0}{pdt} = c_{\mathrm{price}}\frac{d(y_0+y_1+y_2)}{dt}, &
\end{cases} \tag{26}$$

where the price update coefficient c_{price} of the USP corresponds to a unit of time, $Q^{\mathrm{G}}_{i\to 0}$ (or $Q^{\mathrm{G}}_{0\to i}$) are the coefficients reflecting the group-average "willingness" to change the service provider from the LSP i to the USP (or backwards)

after inquiring proximate users, while $Q^{\mathrm{D}}_{i\to 0}$ ($Q^{\mathrm{D}}_{0\to i}$) is the average "dissatisfaction" rate due to a difference between the quality announced by the LSP and the actual experienced quality. Further, $Q_{\varnothing\to 0}$ ($Q_{0\to\varnothing}$) corresponds to a decision on connecting (disconnecting) for the customers without the SIM-cards. Also here, $0 \le y_1 \le D_1$, $0 \le y_2 \le D_2$, $0 \le y_0 \le D_0$, and D_i are the initial shares for the LSPs obtained with either Bertrand or Cournot solutions, while $D_0 = 1 - D_1 - D_2$ are the initially inactive customers.

1) CHANGING SERVICE PROVIDER AFTER PROXIMATE INTERACTION

The current throughput of the customer from the group i is based on equal sharing of bandwidth, that is, $T_i = \frac{B_i\overline{\eta}_i}{Nx_i}$, $i = 1, 2$ or $T_0 = \frac{B_0\overline{\eta}_0}{N(y_0+y_1+y_2)}$, where $\overline{\eta}_i$, $i = 0, 1, 2$ is the average spectral efficiency over the coverage area of one mmWave AAP. We may then calculate $s_i(T_i) = \frac{1}{\frac{b}{T_i}+1} + cT_i$ for each $i = 0, 1, 2$. Denoting these functions as s_i, we continue with deriving the coefficients $Q^{\mathrm{G}}_{i\to 0}$ and $Q^{\mathrm{G}}_{0\to i}$ that capture system dynamics under user "gossiping". We also note that:

$$U(\theta; s_0, p_0) - U(\theta; s_i, p_i)) = \theta(s_0 - s_i) - (p_0 - p_i). \quad (27)$$

Hence, denoting $\frac{p_0-p_i}{s_0-s_i}$ as $\theta_{0,i}$, which defines the ranges of θ, we obtain:

$$U(\theta; s_0, p_0) - U(\theta; s_i, p_i)) > 0, \quad \text{if } \theta > \theta_{0,i}, \quad s_0 > s_i, \quad \text{or } \theta < \theta_{0,i}, \ s_0 < s_i, \quad (28)$$

and a similar expression can be established for $U(\theta; s_0, p_0) - U(\theta; s_i, p_i)) < 0$. Further, in order to average over the range of θ, we integrate p_u ($\Delta U(\theta)$) separately for $\Delta U(\theta) > 0$ and $\Delta U(\theta) < 0$ as:

$$\Delta U(\theta) > 0 : \frac{1}{\theta_{\max}} \int \left(\frac{2}{1 + e^{-c_u(\theta(s_0-s_i)-(p_0-p_i))}} - 1 \right) d\theta = \frac{\theta}{\theta_{\max}} + \frac{1}{\theta_{\max}} \frac{2}{s_0 - s_1} \log(e^{-c_1\theta + c_2} + 1),$$

$$\Delta U(\theta) < 0 : \frac{1}{\theta_{\max}} \int \left(\frac{2}{1 + e^{-c_u(\theta(s_0-s_i)-(p_0-p_i))}} - 1 \right) d\theta = \frac{\theta}{\theta_{\max}} - \frac{1}{\theta_{\max}} \frac{2}{s_0 - s_1} \log(e^{c_1\theta - c_2} + 1). \quad (29)$$

Based on the above range, we may now average over the possible values of θ, and write the following:

$$Q^{\mathrm{G}}_{i\to 0} = \frac{1}{\theta_{\max}} \int_{A_1}^{A_2} \left(\frac{2}{1 + e^{-c_u(\theta(s_0-s_i)-(p_0-p_i))}} - 1 \right) d\theta = \left[\frac{A_2 - A_1}{\theta_{\max}} + \frac{1}{\theta_{\max}} \frac{2}{s_0 - s_1} \log \frac{e^{-c_1A_2+c_2} + 1}{e^{-c_1A_1+c_2} + 1} \right], \quad (30)$$

where $A_1 \ge A_2$ constitute the integration range depending on i as well as on the type of the initial game as per Table 2. If $A \ge A_1$, we say that $Q^{\mathrm{G}}_{i\to 0} = 0$.

TABLE 2. Considered system evaluation parameters.

	$s_0 > s_i$		$s_0 < s_i$ [A]	
	Bertrand	Cournot	Bertrand	Cournot
A_1, LSP 1	$\theta_{\max}$		$\min(\theta_{\max}, \theta_{0,i})$	
A_2, LSP 1	$\max(\theta_{1,2}, \theta_{0,i})$		$\theta_{1,2}$	
A_1, LSP 2	$\theta_{1,2}$	$\theta_{\max}$	$\min(\theta_{1,2}, \theta_{0,i})$	$\min(\theta_{\max}, \theta_{0,i})$
A_2, LSP 2	$\max(\theta_{2,\varnothing}, \theta_{0,i})$		$\theta_{2,\varnothing}$	

[A] If $s_0 = s_i$, a difference between the utilities is only defined by $p_0 - p_i$.

Similarly, $Q^{\mathrm{G}}_{0\to i}$ may be obtained with the only difference that the columns $s_0 > s_i$ and $s_0 < s_i$ swap, and the second line in (29) is utilized for $A_1 \ge A_2$ (otherwise, $Q^{\mathrm{G}}_{0\to i} = 0$):

$$Q^{\mathrm{G}}_{0\to i} = \frac{1}{\theta_{\max}} \int_{A_1}^{A_2} \left(\frac{2}{1 + e^{-c_u(\theta(s_0-s_i)-(p_0-p_i))}} - 1 \right) d\theta = \left[\frac{A_2 - A_1}{\theta_{\max}} + \frac{1}{\theta_{\max}} \frac{2}{s_0 - s_1} \log \frac{e^{-c_1A_2+c_2} + 1}{e^{-c_1A_1+c_2} + 1} \right]. \quad (31)$$

The above expressions cover all four transitions (within the groups 1, 2) for both considered game types. Finally, an inactive customer decides to connect if its utility is above zero (i.e., $\theta > \frac{p_0}{s_0} = \theta_{0,\varnothing}$):

$$Q_{\varnothing\to 0} = \left[\frac{\theta_{2,\varnothing} - \theta_{0,\varnothing}}{\theta_{\max}} + \frac{1}{\theta_{\max}} \frac{2}{s_0 - s_1} \log \frac{e^{-c_1\theta_{2,\varnothing}+c_2} + 1}{e^{-c_1\theta_{0,\varnothing}+c_2} + 1} \right], \quad (32)$$

if $\theta_{0,\varnothing} < \theta_{2,\varnothing}$ or zero, otherwise. Let us also calculate $Q_{0\to\varnothing}$, since this variable and the one above are the only two parameters of interest for the "inactive" market share:

$$Q_{0\to\varnothing} = \left[\frac{\theta_{0,\varnothing}}{\theta_{\max}} - \frac{1}{\theta_{\max}} \frac{2}{s_0 - s_1} \log \frac{e^{c_1\theta_{0,\varnothing}-c_2} + 1}{e^{-c_2} + 1} \right]. \quad (33)$$

2) CHANGING PROVIDER DUE TO CUSTOMER DISSATISFACTION

Dissatisfaction of a customer with the initial subscription to the LSP i depends directly on $U(\theta; s_i(T_i^m), p_i) - U(\theta; s_j, p_j))$, where $j = 0$, i is the index of the current service provider:

$$U(\theta; s_i^m, p_i) - U(\theta; s_j, p_j)) > 0, \quad \text{if } \theta > \theta_{i,j}, \quad s_i^m > s_j, \quad \text{or } \theta < \theta_{i,j}, \ s_i^m < s_j, \ j = 0, i, \quad (34)$$

where $s_i^m = s_i(T_i^m)$ and $\theta_{i,j} = \frac{p_i-p_j}{s_i^m-s_j}$. Here, one may employ similar derivations as above (even a simpler procedure would suffice due to the fact that $\theta_{i,i} = 0$), based on the coefficients from Table 2. The four coefficients in question may be obtained according to:

$$Q^{\mathrm{D}}_{i\to j} = \left[\frac{A_2 - A_1}{\theta_{\max}} + \frac{1}{\theta_{\max}} \frac{2}{s_i^m - s_j} \log \frac{e^{-c_1A_2+c_2} + 1}{e^{-c_1A_1+c_2} + 1} \right], \quad (35)$$

where we do not need to consider the case of negative utility as well as the integral corresponding to the one in

the proximate interaction part (see above). We note that at this point all ten coefficients of interest have been obtained. The corresponding system of differential equations is rather cumbersome to solve analytically, but a numerical solution suffices for our modeling.

E. COOPERATION BETWEEN THE LSPs ("PROXY" FUNCTIONALITY)

We finalize this section by modeling possible cooperation between the LSPs. In particular, we assume that based on a certain long-term agreement, mmWave AAPs (drone cells) of the LSP 1 may assist those of the LSP 2 and the other way around, which has been termed previously the *"proxy" AAP* functionality. As a result, the customers of the LSP i may be served by the closest AAP of either LSP. Since "proxy" handover has to be made transparent for the customer device, we assume the use of the *same frequency band* for such operation, but the system *airtime* is shared as per the actual total number of served customers (see Fig. 2 for details).

We remind that the shares of the customers are denoted as x_i, y_i, as previously. However, these variables correspond to the numbers of devices that may be served by the AAPs of their own LSP. The shares of those that are served by the assisting LSP are denoted as z_i^x, z_i. The average share ϵ of "foreign devices" is calculated according to the geometric probability to place a point into the area when assistance is required. Furthermore, the two average spectral efficiencies $\overline{\eta}_i, i = 1, 2$ are recalculated according to the new AAP deployment. Given these two spectral efficiencies, we may then calculate the throughput of a customer, if the LSP i is assisted by the LSP j, which clearly differs from what we had before. Namely, $T_i^z = \frac{B_j \overline{\eta}_i}{x_i}, (i, j) = (1, 2), (2, 1)$. The operation of the USP does not change when the LSPs cooperate.

Based on the methods similar to those utilized previously, we rewrite the system (26) by adding two more equations that reflect the evolution of z_i:

$$\begin{cases} \frac{dz_1}{dt} = (D_1 - y_1 - z_1)\epsilon\xi\gamma(y_0 + y_1 + y_2) \cdot \tilde{Q}^{\mathrm{G}}_{1\to 0} \\ +(D_1 - y_1 - z_1)\epsilon\xi\alpha_c(1-\gamma) \\ +(D_1 - y_1 - z_1)\epsilon\xi\delta(1-\gamma) \cdot \tilde{Q}^{\mathrm{D}}_{1\to 0} \\ -z_1\xi\gamma(D_1 - y_1 - z_1) \cdot \tilde{Q}^{\mathrm{G}}_{0\to 1} \\ -z_1\xi\alpha_c(1-\gamma) \\ -z_1\xi\delta(1-\gamma) \cdot \tilde{Q}^{\mathrm{D}}_{0\to 1}, \\ \frac{dz_2}{dt} = (D_2 - y_2 - z_2)\epsilon\xi\gamma(y_0 + y_1 + y_2)\tilde{Q}^{\mathrm{G}}_{2\to 0} \\ +(D_2 - y_2 - z_2)\epsilon\xi\alpha_c(1-\gamma) \\ +(D_2 - y_2 - z_2)\epsilon\xi\delta(1-\gamma) \cdot \tilde{Q}^{\mathrm{D}}_{2\to 0} \\ -z_2\xi\gamma(D_2 - y_2 - z_2) \cdot \tilde{Q}^{\mathrm{G}}_{0\to 2} \\ -z_2\xi\alpha_c(1-\gamma) \\ -z_2\xi\delta(1-\gamma) \cdot \tilde{Q}^{\mathrm{D}}_{0\to 2}. \end{cases} \tag{36}$$

Therefore, we obtain the following:

$$\begin{cases} \frac{dy_1}{dt} = (D_1 - y_1 - z_1)(1-\epsilon)\xi\gamma(y_0 + y_1 + y_2) \cdot Q^{\mathrm{G}}_{1\to 0} \\ +(D_1 - y_1 - z_1)(1-\epsilon)\xi\alpha_c(1-\gamma) \\ +(D_1 - y_1 - z_1)(1-\epsilon)\xi\delta(1-\gamma) \cdot Q^{\mathrm{D}}_{1\to 0} \\ -y_1\xi\gamma(D_1 - y_1 - z_1) \cdot Q^{\mathrm{G}}_{0\to 1} \\ -y_1\xi\alpha_c(1-\gamma) \\ -y_1\xi\delta(1-\gamma) \cdot Q^{\mathrm{D}}_{0\to 1}, \\ \frac{dz_1}{dt} = (D_1 - y_1 - z_1)\epsilon\xi\gamma(y_0 + y_1 + y_2) \cdot \tilde{Q}^{\mathrm{G}}_{1\to 0} \\ +(D_1 - y_1 - z_1)\epsilon\xi\alpha_c(1-\gamma) \\ +(D_1 - y_1 - z_1)\epsilon\xi\delta(1-\gamma) \cdot \tilde{Q}^{\mathrm{D}}_{1\to 0} \\ -z_1\xi\gamma(D_1 - y_1 - z_1) \cdot \tilde{Q}^{\mathrm{G}}_{0\to 1} \\ -z_1\xi\alpha_c(1-\gamma) \\ -z_1\xi\delta(1-\gamma) \cdot \tilde{Q}^{\mathrm{D}}_{0\to 1}, \\ \frac{dy_2}{dt} = (D_2 - y_2 - z_2)(1-\epsilon)\xi\gamma(y_0 + y_1 + y_2)Q^{\mathrm{G}}_{2\to 0} \\ +(D_2 - y_2 - z_2)(1-\epsilon)\xi\alpha_c(1-\gamma) \\ +(D_2 - y_2 - z_2)(1-\epsilon)\xi\delta(1-\gamma) \cdot Q^{\mathrm{D}}_{2\to 0} \\ -y_2\xi\gamma(D_2 - y_2 - z_2) \cdot Q^{\mathrm{G}}_{0\to 2} \\ -y_2\xi\alpha_c(1-\gamma) \\ -y_2\xi\delta(1-\gamma) \cdot Q^{\mathrm{D}}_{0\to 2}, \\ \frac{dz_2}{dt} = (D_2 - y_2 - z_2)\epsilon\xi\gamma(y_0 + y_1 + y_2)\tilde{Q}^{\mathrm{G}}_{2\to 0} \\ +(D_2 - y_2 - z_2)\epsilon\xi\alpha_c(1-\gamma) \\ +(D_2 - y_2 - z_2)\epsilon\xi\delta(1-\gamma) \cdot \tilde{Q}^{\mathrm{D}}_{2\to 0} \\ -z_2\xi\gamma(D_2 - y_2 - z_2) \cdot \tilde{Q}^{\mathrm{G}}_{0\to 2} \\ -z_2\xi\alpha_c(1-\gamma) \\ -z_2\xi\delta(1-\gamma) \cdot \tilde{Q}^{\mathrm{D}}_{0\to 2}, \\ \frac{dy_0}{dt} = (D_0 - y_0)\xi\gamma(y_0 + y_1 + y_2 + z_1 + z_2) \cdot Q_{\varnothing\to 0} \\ +(D_0 - y_0)\xi\alpha_c(1-\gamma) \\ -y_0\xi \cdot Q_{0\to\varnothing}, \\ \frac{dp_0}{dt} = c_{\mathrm{price}}\frac{d(y_0+y_1+y_2)}{dt}p. \end{cases} \tag{37}$$

We note that all of the coefficients without a tilde alter according to the updated spectral efficiencies, while those with a tilde are calculated by the analogy with the above, but based on different throughputs.

V. NUMERICAL ANALYSIS OF OUR SYSTEM

A. IMPLEMENTED MODELING ENVIRONMENT

In order to carefully model the dynamic evolution of the system in question, we are not only relying on the above game theoretic tools but also conduct a comprehensive system-level simulation assessment by building own evaluation platform with suitable scaling performance to address our large-scale scenario. The developed simulation platform is based on our previous mmWave study in [51] and additionally implements several unique features that allow it to capture the intricate interactions between our studied entities:

- The simulator utilizes a rescaled framing for medium access control, which enables operation across larger time intervals without affecting the system efficiency.
- The antenna beamforming and body reflection effects are modeled explicitly by applying a mmWave-specific channel model based on the ray-tracing results and real measurements.

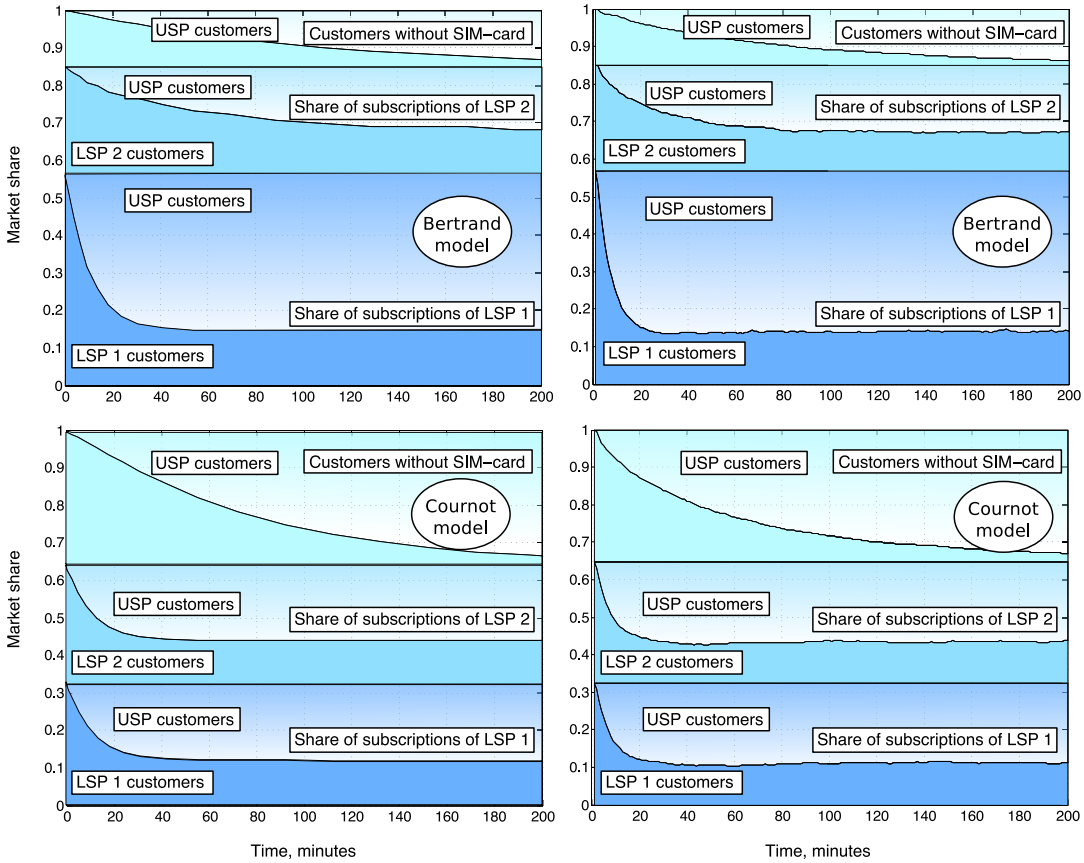

FIGURE 6. Shares of our market in dynamics: the Bertrand (top) and Cournot (bottom) games; analysis (left) and simulation (right).

The investigated short-term dynamics of the aerial mmWave access market is assessed for a characteristic scenario with two LSPs and one USP collocated in a square area of interest with the side length $R = 200$m. Each of these market players has a fleet of mmWave AAPs (drone cells) uniformly deployed over the area, thus forming a regular hexagonal grid. All AAPs of the LSPs are placed at the same altitude $h_i = 15$ m, while the AAPs of the USP occupy $h_0 = 30$ m, which results in expected numbers of 18 and 5 AAPs, respectively. The number of (potentially) active customers is $N = 8,000$ (the total number of participants is $80,000$), who are distributed uniformly across this square area. At every instant of time, each active customer is served by its closest AAP of the service provider it is subscribed to. One unit of time corresponds to one minute. For the complete list of the system settings, we refer to Table 3.

B. QUANTIFYING MARKET DYNAMICS

We begin with investigating the overall dynamics of our subject market, where the initial market shares of the LSPs are determined according to the Bertrand (BM) and the Cournot models (CM) above. These alternatives represent two extreme cases of possible market alignment corresponding to the differentiated vs. identical product offers, respectively, and lead to dissimilar conclusions on system performance.

Since the user utility is assumed to be linear with respect to the price as well as the quality $s(T)$, we impose that $s(T)$ has a similar structure to what service providers use in real markets. Accordingly, we let our quality $s(T)$ translate into:

$$s(T) = \frac{aT}{T+b} + cT, \tag{38}$$

where a, b, and c are the coefficients that may be obtained from real network operator prices via the linear regression.

Our first result addresses the case when two independent LSPs observe the consequences of the USP intrusion into "their" equilibrium market and capture the temporal evolution of the *market shares* illustrated here for the scenario with $\alpha_c = 0.0083$ (equivalent to a period of 2 hours), $\gamma = 0.05$, $\delta = 0.1$, and the initial price $p_0 = p_2/2$. To this end, Fig. 6 indicates time (in minutes) along the horizontal axis, while the vertical axis reports the distribution of the shares of the customers for the market players. On the right side of this plot, we append our simulation results to validate the analysis on the left side.

The key difference that is revealed when comparing the BM and the CM cases of the initial-stage modeling is in their respective market shares (that is, at time $t = 0$). For the CM, the LSP 1 and the LSP 2 have equal shares of subscribers (i.e., 0.33), while the remaining market share comprises the customers with no SIM-cards (not connected to either LSP). In contrast, for the BM, the LSP 1 has a larger initial market

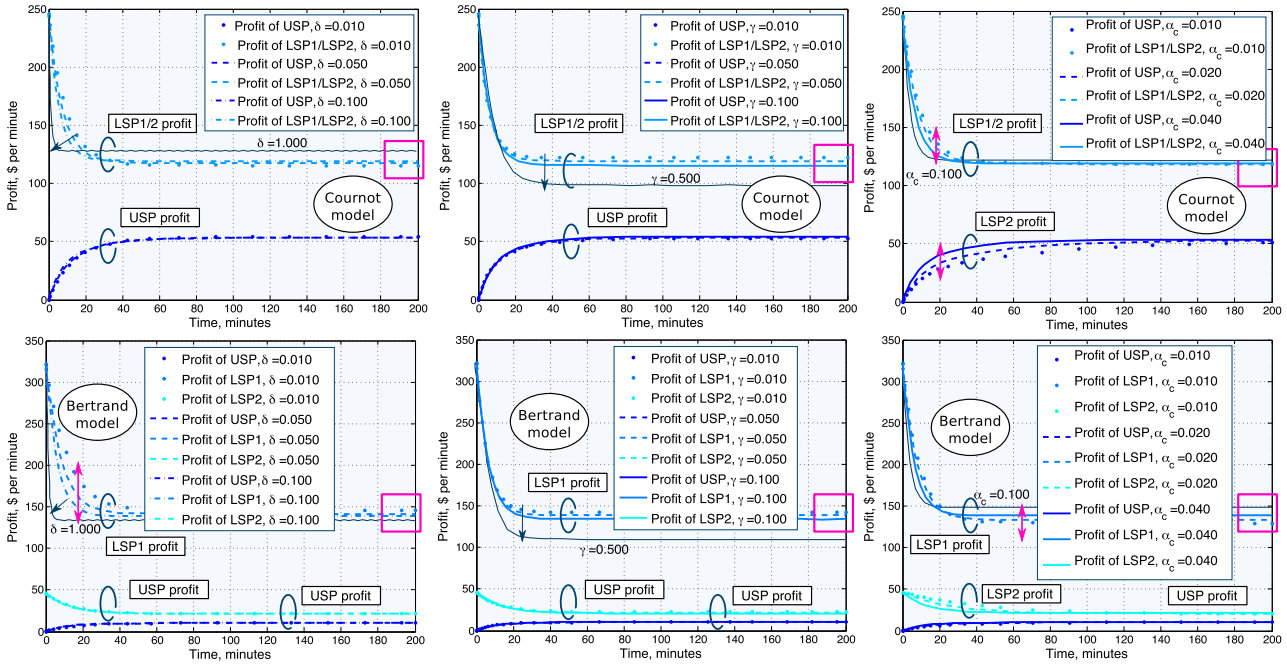

FIGURE 7. **Profit of our main market players in dynamics: the Cournot (top) and Bertrand (bottom) games; with "dissatisfaction" (left), "gossiping" (middle), and "curiosity" (right) factors.**

TABLE 3. **System evaluation parameters.**

Name	Description/definition	Value		
R	Area of interest	200m		
μ_0	Density of devices	0.2 per m^2		
μ	Density of users	2 per m^2		
h_b	Average body height	1.7m		
r_b	Average body radius	0.2m		
h_d	Average device elevation	1.2m		
ϕ	Half of aperture	10^o		
$\beta_{\max}$	Maximum beam inclination	60^o		
α	Antenna "viewing angle"	270^o		
h_i	AAP altitude	15m	15m	30m
B_i	Bandwidth [A]	2GHz	2GHz	6GHz
p_{tx}	Transmit power	200 mW		
f_i	Frequency	28GHz	28GHz	60GHz
N_0	Noise plus interference	-80dBm		
G_{NLOS}	Reflected beam path decrease	-30dB		
$\text{SNR}_{\max}$	Maximum SNR	20dB		
$\theta_{\max}$	Maximum "taste" [B]	234.03		
T^m	Maximum throughput	100		
a, b, c	Quality function parameters	(12.3600, 0.5619, 0.0098)		
ν	Costs per unit of demand [C]	0.0647		
γ	"Gossiping" factor	0.05		
α_c	"Curiosity" factor	0.05		
δ	"Dissatisfaction" factor	0.1		
c_{price}	USP price update	0.1		
c_u	Utility "impact" coefficient	0.1		

[A] Maximum bandwidth purchased by the LSP may be decreased according to the difference in the optimal costs at the initial-stage game. For the final throughput, the value in Hz is multiplied by 0.5 to obtain the "effective bandwidth".
[B] Derived under the assumption that the "richest" customer is ready to pay not more than 200$ per month (i.e., 0.46 cents per minute).
[C] Derived assuming that the annual license costs 50 million dollars per 2 GHz.

share (i.e., 0.58) and the LSP 2 has a smaller one (i.e., 0.29). Further, we observe that the evolution of these shares has similar trends for both cases: the USP can acquire significant shares of the market not only by activating the customers with no SIM-card but also by winning the customers of the LSPs. The dynamics of this process changes over time by converging to a stable balance for the LSPs in about 1 hour. Given the excellent match between our analytical and simulation results, in the remainder of this section, we focus only on the findings of our mathematical analysis.

We continue by investigating the *profit evolution* (including spectrum costs and fees paid by the customers). To this end, Fig. 7 studies the impact of such factors as consumer "gossiping", "curiosity", and "dissatisfaction" over a realistic range of values (lighter curves). We also report more "extreme" results (darker curves) to highlight the potential range of the profit. Our first observation is that only user "curiosity" has a significant effect on the lowest-profitable USP and the second-profitable LSP 2 (in the BM). Specifically, it increases the profit of an LSP with the growing α_c as well as alters the convergence time. The latter trend holds for the "dissatisfaction" factor as well, but an increase in δ for the BM (but not the CM) results in a lower profit of the highest-price LSP 1 (since both the announced quality level and the price are higher). This reveals an important difference between the BM and the CM in terms of the USP "intrusion". The last remaining "gossiping" factor γ may significantly lower the profit of both LSPs (as shown by the "extreme" line), which implies that the more the customers interact, the higher utility they can achieve. This feature – in a way similar to implicit customer cooperation – is clearly beneficial for them, and hence suggests a hypothesis on that some level of cooperation between the LSPs may also bring value. Therefore, we shift our focus to the cooperation of the LSPs in what follows.

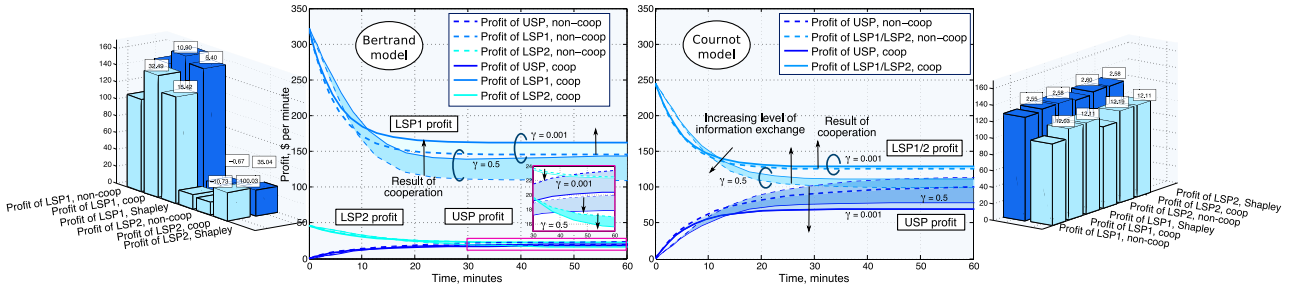

FIGURE 8. Consequences of the LSP cooperation in dynamics: the Bertrand (left) and Cournot (right) games; arrows follow changes in profit due to cooperation.

C. EFFECTS OF THE LSP COOPERATION

In this subsection, we characterize the market impact of cooperation between the LSPs, which aims to help serve their customers more efficiently. Accordingly, Fig. 8 illustrates the temporal evolution of the LSP profits for the two extreme values (0.001 and 0.5) of the "gossiping" factor γ with and without cooperation. In the plot, an increase in the profit due to the LSP cooperation is highlighted by the filled areas. Interestingly, we observe differences between the short- and the long-term dynamics for both the BM and the CM cases (see, e.g., $t < 8$ and $t > 8$). It becomes apparent that cooperation always benefits the LSP 1, while the LSP 2 wins only for the CM. On the contrary, for the BM, cooperation may result in a lower LSP 2 profit, which suggests the importance of financial compensation from the winning LSP 1. From the theoretical viewpoint, it translates into the need for a fair utility sharing. Hence, the aggregate profit could be split between the LSPs according to, e.g., the Shapley value to enforce fairness of cooperation as it is shown by the bar graphs in Fig. 8.

VI. SUMMARY AND CONCLUSIONS

The unique modeling framework proposed in this paper makes a decisive step toward understanding the novel market around the mmWave access systems as part of the 5G/5G+ landscape. The unexpected and temporary events featuring masses of people constitute particularly challenging study cases in this area because of unprecedented bandwidth requirements that can only be satisfied with emerging radio technologies (e.g., aerial mmWave access points that employ UAV-mounted small cells). In this paper, we provide a systematic performance characterization of competition and cooperation behavior of dissimilar aerial mmWave access suppliers by modeling a vertically differentiated market, where customers have different preferences for access service quality. We construct the Nash equilibrium for the initial market competition and conduct an assessment of short-term market dynamics, where licensed-band service providers (LSPs) may cooperate to improve their competitive positions against an unlicensed-band counterpart intruding the market.

To comprehensively model the competition among dissimilar players in the subject market, we apply the Bertrand and Cournot games, which lead to drastically different performance results. More specifically, in the Cournot model, we observe that the market is equally shared between the LSPs, with subsequent equal profit sharing. Here, the total market profit turns out to be higher than that in the Bertrand model, where instead a clear differentiation between the LSPs occurs in terms of profits. The other side of the coin is that the Cournot model leads to a lower surplus, as well as to a smaller number of served customers, which may become negative factors with respect to long-term customer loyalty.

Another lesson learned as a result of our analysis is that the factors of customer behavior, such as "gossiping", "curiosity", and "dissatisfaction", yield various consequences on the access market dynamics and the resulting profits, and depend on whether the Bertrand or Cournot game is played initially. Whenever the customers enjoy high levels of interaction with each other, they can collectively improve their utility by dynamically adapting their service provider choices. When that happens, we study the presence of the USP (unlicensed-band service provider) on the market in question, mindful of customer adaptation dynamics. Competing against the USP, the LSPs may also engage in mutual cooperation to better satisfy the customer demands and, thus, increase their profits. Here, the need for a fair sharing of the resulting profit is essential to guarantee benefits for both cooperating LSPs, and we adopt the Shapley value for that purpose.

While this study focuses on the uniform distribution of the taste parameter and linear costs of quality improvement, future case studies may include, for example, a more realistic description of user preferences, including customer utility functions and their distribution. Another prospective scenario may be found in relaxing the assumption of one subscription plan per provider as the latter typically offers multiple differentiated products, and the new market structure is to be addressed separately.

Concluding this work, we are convinced that our first-hand game theoretic modeling conducted in this paper should become a useful reference point for future discussions on the dynamic 5G market environments. Multiple new research directions may stem from our present contribution along the lines of dynamic deployment and operation optimization of the aerial access points, profit maximization studies across a range of service and business models that enable customer-driven decision making, as well as further

game-theoretic analysis of alternative market settings and player strategies.

APPENDIX

A. BLOCKAGE PROBABILITY ILLUSTRATION

Let us establish here the probability of blockage by a cylindric object, if the device is located at the distance d from the AAP. We assume that the mmWave radio "shadow" is equivalent in its shape and size to the one that visible light creates, and that the LOS is blocked *iff* the axis of symmetry of the radio beam is blocked (see SC in Fig. 9.b). Then, the closest blocking body may be located at the point A, while the device is placed at the point B, and a hatched region indicates the locus of centers of all the possible blockers in Fig. 9.c of area $S_b \approx 2r_b \cdot AB$ (we assume that no center can be placed closer than r_b). Here, $2r_b$ is the width of the cylinder representing the human body, $r_{\max} = d\tan\phi$, ϕ is half of the beam angle, and AB is the longest distance between the device and its blocker. The latter may be calculated based on the properties of similar triangles:

$$\frac{h-h_d}{d} = \frac{h_b-h_d}{AB-r_b},$$

where h, h_b, and h_d are the altitude of AAP, the blocker height, and the device elevation, respectively. Given the above, we obtain:

$$AB = d\frac{h_b-h_d}{h-h_d} + r_b \Rightarrow S_b = 2r_b \cdot d\left(\frac{h_b-h_d}{h-h_d}\right).$$

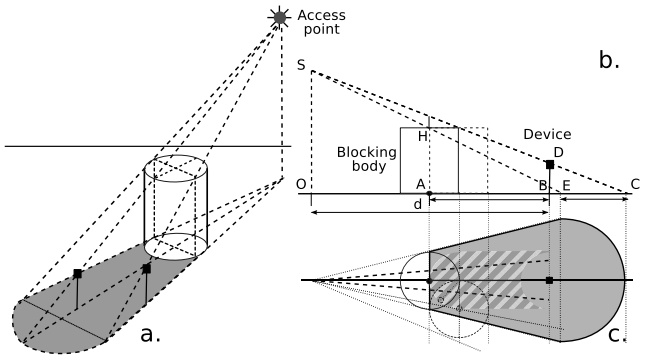

FIGURE 9. Illustration of mmWave blockage probability.

We note that the latter expression is valid if the center of the blocker is located between the projection O and the blocked device, and we disregard the cases when the shadow is "egg-shaped". Due to our assumption on the PPP of the blockers, the probability of not being blocked may be produced as follows:

$$\Pr\{\text{no blockers in the area}\} \approx e^{-\mu\cdot 2r_b\left(d\frac{h_b-h_d}{h-h_d}\right)},$$

where μ is the density of all the participants on the ground of the large-scale event in question.

B. AREA OF BEAM ON THE GROUND

Proposition 3: Consider an AAP at the altitude h, its closest device, and a device located at the distance d. Then, for the beam aperture 2ϕ, the area covered by the beam under the AAP equals $S_0 = \pi\,(h\tan(\phi))^2$. Further, the ratio between the areas S_0 and $S(d)$, which is produced by the device located at the distance d, equals:

$$\frac{S(d)}{S_0} = \frac{\cos(\phi)}{\sqrt{\cos^2(\phi) - \frac{d^2}{d^2+h^2}}}. \tag{39}$$

Proof: Assuming that the area directly under the AAP is a circle of radius a, so that $S_0 = \pi a^2$, the area S may be established as $\pi a \cdot b = \pi a^2/\sqrt{1-e^2}$, where $a = h\tan(\phi)$ and b are the minor and the major radius of the ellipse, respectively, e is its eccentricity, and ϕ is a half of the beam aperture. We note that the eccentricity of the ellipse that represents the result of conic section by a plane is given by $e = \cos\psi/\cos\phi$, where ψ is the angle between the plane (in our case, the ground) and the cone symmetry axis, that is:

$$\tan(\psi) = \frac{h}{d} \Rightarrow \cos^2(\psi) = \frac{1}{1+\frac{h^2}{d^2}}. \tag{40}$$

Therefore, we may obtain the following ratio:

$$\frac{S}{S_0} = \frac{1}{\sqrt{1-\frac{\frac{1}{1+\frac{h^2}{d^2}}}{\cos^2(\phi)}}} = \frac{\cos(\phi)}{\sqrt{\cos^2(\phi)-\frac{d^2}{d^2+h^2}}}. \tag{41}$$

□

C. PROBABILITY OF THE REFLECTED PATH

We assume that in case the LOS link does not exist, the mmWave connection between the AAP and its associated device may be supported via a signal reflected from, e.g., another human body. Excluding the blocked device and its possible blocker, we need to estimate whether any other human body is present within the area covered by the directed beam. Utilizing our assumption on the PPP for the devices, we may establish the probability of NLOS path as follows:

$$\begin{aligned} q_{\text{NLOS}}(d) &= \Pr\{\text{NLOS at } d\} \\ &= -exp\left(-\mu\frac{\pi\,(h\tan(\phi))^2\cos(\phi)}{\sqrt{\cos^2(\phi)-\frac{d^2}{d^2+h^2}}}\right). \end{aligned} \tag{42}$$

REFERENCES

[1] *The 3rd Generation Partnership Project (3GPP) Website*. Accessed: Jun. 2019. [Online]. Available: http://www.3gpp.org/release-16

[2] "Designing 5G NR: The 3GPP Release-15 global standard for a unified, more capable 5G air interface," Qualcomm, San Diego, CA, USA, White Paper, Sep. 2018. [Online]. Available: https://www.qualcomm.com/media/documents/files/the-3gpp-release-15-5g-nr-design.pdf

[3] "Expanding the 5G NR ecosystem: 5G NR roadmap in 3GPP Release 16 and beyond," Qualcomm, San Diego, CA, USA, White Paper, Sep. 2018. [Online]. Available: https://www.qualcomm.com/documents/expanding-5g-nr-ecosystem-and-roadmap-3gpp-rel-16-beyond
[4] *Standard for Information Technology–Telecommunications and Information Exchange Between Systems Local and Metropolitan Area Networks–Specific Requirements - Part 11: Wireless LAN Medium Access Control (MAC) and Physical Layer (PHY) Specifications Amendment: Light Communications*, IEEE Standard P802.11bb, 2017.
[5] *Status of Project IEEE 802.11ay. Enhanced Throughput for Operation in License-Exempt Bands Above 45 GHz*, IEEE Standard P802.11, 2018. [Online]. Available: http://www.ieee802.org/11/Reports/tgay_update.htm
[6] R. Baldemair, T. Irnich, K. Balachandran, E. Dahlman, G. Mildh, and Y. Selén, S. Parkvall, M. Meyer, and A. Osseiran, "Ultra-dense networks in millimeter-wave frequencies," *IEEE Commun. Mag.*, vol. 53, no. 1, pp. 202–208, Jan. 2015.
[7] S. Andreev, V. Petrov, M. Dohler, and H. Yanikomeroglu, "Future of ultra-dense networks beyond 5G: Harnessing heterogeneous moving cells," *IEEE Commun. Mag.*, to be published.
[8] I. Bor-Yaliniz and H. Yanikomeroglu, "The new frontier in RAN heterogeneity: Multi-tier drone-cells," *IEEE Commun. Mag.*, vol. 54, no. 11, pp. 48–55, Nov. 2016.
[9] D. Floreano and R. J. Wood, "Science, technology and the future of small autonomous drones," *Nature*, vol. 521, no. 7553, pp. 460–466, May 2015.
[10] R. L. Aguiar, "White paper for research beyond 5G (final edit)," Networld, Germany, Tech. Rep., Jan. 2016. [Online]. Available: https://networld2020.eu/wp-content/uploads/2016/03/B5G-Vision-for-Researchv-1.1b_final-and-approved.pdf
[11] *Federal Aviation Administration*. Accessed: Jun. 2019. [Online]. Available: https://www.faa.gov/uas/
[12] The METIS 2020 Project. (Apr. 2015). *Updated Scenarios, Requirements KPIs for 5G Mobile Wireless System With Recommendations for Future Investigations*. [Online]. Available: https://metis2020.com/wp-content/uploads/deliverables/METIS_D1.5_v1.pdf
[13] M. Mozaffari, W. Saad, M. Bennis, and M. Debbah, "Unmanned aerial vehicle with underlaid device-to-device communications: Performance and tradeoffs," *IEEE Trans. Wireless Commun.*, vol. 15, no. 6, pp. 3949–3963, Jun. 2016.
[14] Z. Xiao, P. Xia, and X.-G. Xia, "Enabling UAV cellular with millimeter-wave communication: Potentials and approaches," *IEEE Commun. Mag.*, vol. 54, no. 5, pp. 66–73, May 2016.
[15] A. Ghosh, T. A. Thomas, M. C. Cudak, R. Ratasuk, P. Moorut, F. W. Vook, T. S. Rappaport, S. Sun, G. R. MacCartney, and S. Nie, "Millimeter-wave enhanced local area systems: A high-data-rate approach for future wireless networks," *IEEE J. Sel. Areas Commun.*, vol. 32, no. 6, pp. 1152–1163, Jun. 2014.
[16] X. Cao, P. Yang, M. Alzenad, X. Xi, D. Wu, and H. Yanikomeroglu, "Airborne communication networks: A survey," *IEEE J. Sel. Areas Commun.*, vol. 36, no. 9, pp. 1907–1926, Sep. 2018.
[17] L. Gupta, R. Jain, and G. Vaszkun, "Survey of important issues in UAV communication networks," *IEEE Commun. Surveys Tuts.*, vol. 18, no. 2, pp. 1123–1152, 2nd Quart., 2016.
[18] S. Hayat, E. Yanmaz, and R. Muzaffar, "Survey on unmanned aerial vehicle networks for civil applications: A communications viewpoint," *IEEE Commun. Surveys Tuts.*, vol. 18, no. 4, pp. 2624–2661, 4th Quart., 2016.
[19] G. Owen, *Game Theory*. San Diego, CA, USA: Academic, 1995.
[20] Z. Han, D. Niyato, W. Saad, T. Başar, and A. Hjørungnes, *Game Theory in Wireless and Communication Networks: Theory, Models, and Applications*. Cambridge, U.K.: Cambridge Univ. Press, 2011.
[21] K. Akkarajitsakul, E. Hossain, D. Niyato, and D. I. Kim, "Game theoretic approaches for multiple access in wireless networks: A survey," *IEEE Commun. Surveys Tuts.*, vol. 13, no. 3, pp. 372–395, 3rd Quart., 2011.
[22] D. T. Hoang, X. Lu, D. Niyato, P. Wang, D. I. Kim, and Z. Han, "Applications of repeated games in wireless networks: A survey," *IEEE Commun. Surveys Tuts.*, vol. 17, no. 4, pp. 2102–2135, 4th Quart., 2015.
[23] M. E. Mkiramweni, C. Yang, J. Li, and Z. Han, "Game-theoretic approaches for wireless communications with unmanned aerial vehicles," *IEEE Wireless Commun.*, vol. 25, no. 6, pp. 104–112, Dec. 2018.
[24] S. Ren, J. Park, and M. van der Schaar, "Entry and spectrum sharing scheme selection in femtocell communications markets," *IEEE/ACM Trans. Netw.*, vol. 21, no. 1, pp. 218–232, Feb. 2013.
[25] D. Niyato and E. Hossain, "Competitive pricing for spectrum sharing in cognitive radio networks: Dynamic game, inefficiency of Nash equilibrium, and collusion," *IEEE J. Sel. Areas Commun.*, vol. 26, no. 1, pp. 192–202, Jan. 2008.
[26] A. Shaked and J. Sutton, "Relaxing price competition through product differentiation," *Rev. Econ. Stud.*, vol. 49, no. 1, pp. 3–13, 1982.
[27] J. J. Gabszewicz and J.-F. Thisse, "Price competition, quality and income disparities," *J. Econ. Theory*, vol. 20, no. 3, pp. 340–359, 1979.
[28] A. Shaked and J. Sutton, "Natural oligopolies," *Econometrica*, vol. 51, pp. 1469–1483, 1983.
[29] M. Motta, "Endogenous quality choice: Price vs. Quantity competition," *J. Ind. Econ.*, vol. 41, no. 2, pp. 113–131, 1993.
[30] G. Bonanno, "Vertical differentiation with Cournot competition," *Economic Notes*, vol. 15, no. 2, pp. 68–91, 1986.
[31] W. H. Sandholm, "Pairwise comparison dynamics and evolutionary foundations for Nash equilibrium," *Games*, vol. 1, no. 1, pp. 3–17, 2009.
[32] S. H. Tijs and T. S. H. Driessen, "Game theory and cost allocation problems," *Manage. Sci.*, vol. 32, no. 8, pp. 1015–1028, 1986.
[33] L. S. Shapley, "A value for n-person games," *Contributions Theory Games*, vol. 2, no. 28, pp. 307–317, 1953.
[34] L. Militano, M. Nitti, L. Atzori, and A. Iera, "Enhancing the navigability in a social network of smart objects: A Shapley-value based approach," *Comput. Netw.*, vol. 103, pp. 1–14, Jul. 2016.
[35] L. Rose, E. V. Belmega, W. Saad, and M. Debbah, "Pricing in heterogeneous wireless networks: Hierarchical games and dynamics," *IEEE Trans. Wireless Commun.*, vol. 13, no. 9, pp. 4985–5001, Sep. 2014.
[36] K. Zhu, E. Hossain, and D. Niyato, "Pricing, spectrum sharing, and service selection in two-tier small cell networks: A hierarchical dynamic game approach," *IEEE Trans. Mobile Comput.*, vol. 13, no. 8, pp. 1843–1856, Aug. 2014.
[37] J. Hofbauer and K. Sigmund, "Evolutionary game dynamics," *Bull. Amer. Math. Soc.*, vol. 40, no. 4, pp. 479–519, 2003.
[38] J. W. Weibull, *Evolutionary Game Theory*. Cambridge, MA, USA: MIT, 1997.
[39] O. Korcak, G. Iosifidis, T. Alpcan, and I. Koutsopoulos, "Competition and regulation in a wireless operator market: An evolutionary game perspective," in *Proc. Int. Conf. Netw. Games, Control Optim. (NetGCooP)*, Nov. 2012, pp. 17–24.
[40] D. Niyato and E. Hossain, "Dynamics of network selection in heterogeneous wireless networks: An evolutionary game approach," *IEEE Trans. Veh. Technol.*, vol. 58, no. 4, pp. 2008–2017, May 2009.
[41] W. Khawaja, O. Ozdemir, and I. Guvenc, "UAV air-to-ground channel characterization for mmWave systems," in *Proc. IEEE 86th Veh. Technol. Conf. (VTC-Fall)*, Sep. 2017, pp. 1–5.
[42] A. A. Khuwaja, Y. Chen, N. Zhao, M.-S. Alouini, and P. Dobbins, "A survey of channel modeling for UAV communications," *IEEE Commun. Surveys Tuts.*, vol. 20, no. 4, pp. 2804–2821, 4th Quart., 2018.
[43] K. Lancaster, "The economics of product variety: A survey," *Marketing Sci.*, vol. 9, no. 3, pp. 189–206, 1990.
[44] E. Gal-Or, "Quality and quantity competition," *Bell J. Econ.*, vol. 14, no. 2, pp. 590–600, 1983.
[45] P. Milgrom and J. Roberts, "Price and advertising signals of product quality," *J. Political Economy*, vol. 94, no. 4, pp. 796–821, 1986.
[46] R. E. Kihlstrom and M. H. Riordan, "Advertising as a signal," *J. Political Economy*, vol. 92, no. 3, pp. 427–450, 1984.
[47] M. Bennis, J. Lara, and A. Tolli, "Non-cooperative operators in a game-theoretic framework," in *Proc. IEEE 19th Int. Symp. Pers., Indoor Mobile Radio Commun.*, Sep. 2008, pp. 1–5.
[48] M. B. Vandenbosch and C. B. Weinberg, "Product and price competition in a two-dimensional vertical differentiation model," *Marketing Sci.*, vol. 14, no. 2, pp. 224–249, 1995.
[49] O. Galinina, L. Militano, A. Orsino, S. Andreev, G. Araniti, A. Iera, and Y. Koucheryavy, "Comparing customer taste distributions in vertically differentiated mobile service markets," in *Proc. Int. Conf. Game Theory Netw.* Cham, Switzerland: Springer, 2017, pp. 141–153.
[50] *Propagation Data Prediction Methods for Design Terrestrial Broadband Millimetric Radio Access Systems Operating in a Frequency Range About 20-50 GHz*, document Rec. ITU-R 3–1410, 2005.
[51] O. Galinina, A. Pyattaev, K. Johnsson, A. Turlikov, S. Andreev, and Y. Koucheryavy, "Assessing system-level energy efficiency of mmwave-based wearable networks," *IEEE J. Sel. Areas Commun.*, vol. 34, no. 4, pp. 923–937, Apr. 2016.

OLGA GALININA received the B.Sc. and M.Sc. degrees in applied mathematics from the Department of Applied Mathematics, Faculty of Mechanics and Physics, St. Petersburg State Polytechnical University of Peter the First, Russia, and the Ph.D. degree from the Tampere University of Technology, in 2015. She is currently a Postdoctoral Researcher with the Unit of Electrical Engineering, Tampere University. Her research interests include applied mathematics and statistics, queueing theory and its applications, wireless networking and energy efficient systems, and machine-to-machine and device-to-device communication.

LEONARDO MILITANO received the M.Sc. degree in telecommunications engineering and the Ph.D. degree in telecommunications engineering from the University Mediterranea of Reggio Calabria, in 2006 and 2010, respectively, where he is currently an Assistant Professor. He was a Visiting Ph.D. Student with the Mobile Device Group, University of Aalborg, Denmark. His major research interests include wireless network optimization, user and network cooperation, device-to-device communications, and game theory.

SERGEY ANDREEV received the Specialist and Cand.Sc. degrees from SUAI, in 2006 and 2009, respectively, and the Ph.D. degree from TUT, in 2012. He is currently an Assistant Professor of communications engineering and an Academy Research Fellow with Tampere University, Finland. Since 2018, he has also been a Visiting Senior Research Fellow with the Centre for Telecommunications Research, King's College London, U.K. He has coauthored more than 200 published research works on the intelligent IoT, mobile communications, and heterogeneous networking.

ALEXANDER PYATTAEV received the B.Sc. degree from the St. Petersburg State University of Telecommunications, Russia, and the M.Sc. and Ph.D. degrees from TUT. He is currently a Postdoctoral Researcher with the Unit of Electrical Engineering, Tampere University. He has publications on a variety of networking-related topics in internationally recognized venues, as well as several technology patents. His current research interests include future wireless networks: shared spectrum access, smart RAT selection, and flexible and adaptive topologies.

KERSTIN JOHNSSON received the Ph.D. degree in electrical engineering from Stanford University. She is currently a Senior Research Scientist with the Wireless Communications Laboratory, Intel Corporation, where she conducts research on MAC, networks, and application layer optimizations that improve the mobile client experience while reducing wireless operator costs. She has more than ten-year experience in the wireless industry. She has authored numerous publications. She holds patents in the field of wireless communications.

ANTONINO ORSINO received the B.Sc. degree in telecommunication engineering from the University Mediterranea of Reggio Calabria, Italy, in 2009, and the M.Sc. degree from the University of Padova, Italy, in 2012. He is currently pursuing the Ph.D. degree with the DIIES Department, University Mediterranea of Reggio Calabria. He is also a Visiting Researcher with the Tampere University of Technology, Finland. His current research interests include device-to-device and machine-to-machine communications in 4G/5G cellular systems. He has served as a Reviewer for several major IEEE conferences and journals.

GIUSEPPE ARANITI received the Laurea and Ph.D. degrees in electronic engineering from the University Mediterranea of Reggio Calabria, in 2000 and 2004, respectively, where he is currently an Assistant Professor of telecommunications. His major areas of research include personal communications systems, enhanced wireless and satellite systems, traffic and radio resource management, multicast and broadcast services, and device-to-device and machine-type communications over 4G/5G cellular networks.

ANTONIO IERA graduated in computer engineering from the University of Calabria, Italy, in 1991, the Master Diploma degree in information technology from CEFRIEL/Politecnico di Milano, Italy, in 1992, and the Ph.D. degree from the University of Calabria, in 1996. Since 1997, he has been with the University of Mediterranea of Reggio Calabria, where he is currently a Full Professor of telecommunications and the Director of the Laboratory for Advanced Research into Telecommunication Systems. His research interests include next-generation mobile and wireless systems, RFID systems, and the Internet of Things.

MISCHA DOHLER is currently a Full Professor in wireless communications with King's College London, the Head of the Centre for Telecommunications Research, a Co-Founder and Member of the Board of Directors of the smart city pioneer Worldsensing, a Distinguished Lecturer of the IEEE, and the Editor-in-Chief of *Wiley Transactions on Emerging Telecommunications Technologies* and EAI *Transactions on the Internet of Things*. He is a frequent keynote, panel, and tutorial speaker. He has pioneered several research fields, contributed to numerous wireless broadband, IoT/M2M, and cyber security standards, holds 12 patents, has organized and chaired numerous conferences, has more than 200 publications, and has authored several books. He acts as a policy, technology, and entrepreneurship adviser. He has talked at TEDx and had coverage on TV and radio.

YEVGENI KOUCHERYAVY received the Ph.D. degree from TUT, in 2004. He is currently a Professor with the Unit of Electrical Engineering, Tampere University. He has authored numerous publications in the field of advanced wired and wireless networking and communications. His current research interests include various aspects in heterogeneous wireless communication networks and systems, the Internet of Things and its standardization, as well as nanocommunications. He is an Associate Technical Editor of the *IEEE Communications Magazine* and an Editor of the IEEE COMMUNICATIONS SURVEYS AND TUTORIALS.